

Causal effects on non-terminal event time with application to antibiotic usage and future resistance

Tamir Zehavi¹, Uri Obolski², Michal Chowers^{3,4}, Daniel Nevo^{1*}

¹Department of Statistics and Operations Research, Faculty of Exact Sciences, Tel Aviv University, Tel Aviv, Israel

²Department of Epidemiology and Preventive Medicine, School of Public Health, Faculty of Medical and Health Sciences, Tel Aviv University, Tel Aviv, Israel

³Gray Faculty of Medical and Health Sciences, Tel Aviv University

⁴Meir Medical Center, Kfar Saba, Israel

Abstract

Comparing future antibiotic resistance levels resulting from different antibiotic treatments is challenging because some patients may survive only under one of the antibiotic treatments. We embed this problem within a semi-competing risks approach to study the causal effect on resistant infection, treated as a non-terminal event time. We argue that existing principal stratification estimands for such problems exclude patients for whom a causal effect is well-defined and is of clinical interest. Therefore, we present a new principal stratum, the infected-or-survivors (ios). The ios is the subpopulation of patients who would have survived or been infected under both antibiotic treatments. This subpopulation is more inclusive than previously defined subpopulations. We target the causal effect among these patients, which we term the feasible-infection causal effect (FICE). We develop large-sample bounds under novel assumptions, and discuss the plausibility of these assumptions in our application. As an alternative, we derive FICE identification using two illness-death models with a bivariate frailty random variable. These two models are connected by a cross-world correlation parameter. Estimation is performed by an expectation-maximization algorithm followed by a Monte Carlo procedure. We apply our methods to detailed clinical data obtained from a hospital setting.

*danielnevo@tauex.tau.ac.il. TZ and DN were supported by a grant from the Tel Aviv University Center for AI and Data Science (TAD) and by ISF grant 827/21. UO was supported by ISF grant 1286/21.

1 Introduction

Antibiotic resistance, the ability of bacteria to survive in an environment containing antibiotic drugs, is a major public-health threat, and has been linked to approximately 4.95 million annual deaths ([Murray et al. 2022](#), [Okeke et al. 2024](#)). The increasing rates of antibiotic resistance have raised substantial concerns about the future effectiveness of antibiotic treatments ([Ventola 2015](#), [Okeke et al. 2024](#)). Prior antibiotic usage has been repeatedly correlated with increasing antibiotic resistance rates ([Bell et al. 2014](#), [Gladstone et al. 2021](#), [Baraz et al. 2023](#)), presumably as a result of evolutionary forces selecting for antibiotic resistant bacteria. As these findings might be confounded by many factors, causal effects of antibiotic treatment on subsequent antibiotic resistance are generally understudied.

The WHO AWaRe (Access, Watch, Reserve) antibiotic book ([WHO 2017](#)) offers recommendations on antibiotic selection, dosing, route of administration, and treatment duration for common clinical infections in both children and adults. *Access* antibiotics have a narrow spectrum of activity, and they generally convey low future antibiotic resistance potential. *Watch* antibiotics are broader-spectrum antibiotics, generally leading to higher future resistance, and are recommended as first-choice options for patients with more severe clinical presentations or for infections where the causative pathogens are more likely to be resistant to Access antibiotics. Finally, *Reserve* antibiotics are those meant to be mainly used as a last-resort antibiotics for severe infections that are resistant to multiple antibiotics. While the consequences of antibiotic choice on future resistance is widely acknowledged, only a few studies formally study this causal question ([Chowers et al. 2022](#), [Saciuk et al. 2025](#)). Further methodological advances are essential to enable quantitative estimation of the causal effect of prescribing antibiotics so it is incorporated into clinical decision-making.

The comparison between antibiotic treatments with respect to future antibiotic resistance is complicated by the fact that some patients may only survive under one of the antibiotic

treatments. We embed this problem within the semi-competing risks (SCR) data structure, also termed the illness-death model (Fix & Neyman 1951, Xu et al. 2010). SCR data arise when studying times to two events, a non-terminal event and a terminal event. The terminal event can occur after the non-terminal event, but not vice versa. In our motivating example, death is a terminal event that precludes the occurrence of a future resistant bacterial infection. However, death is possible after a resistant bacterial infection, sometimes as a direct consequence of the newly acquired infection. When studying treatment effects on SCR data, challenges arise in defining and interpreting standard causal effects (Nevo & Gorfine 2022), similarly to the closely-related truncation by death problem (Zhang & Rubin 2003, Ding & Lu 2017, Zehavi & Nevo 2023, Tong et al. 2025).

Several regression-based models have been proposed for SCR data, aiming to extract different information and tackle various challenges (Peng & Fine 2007, Hsieh & Huang 2012, Lee et al. 2015, Nevo et al. 2022, Gorfine et al. 2021, Kats & Gorfine 2023). These approaches directly model the realized event times distribution, and are not built upon a non-parametric assumption-free definition of causal effects.

The causal effect of different antibiotic treatments on time to resistant infection is challenging to define. A simple comparison between the cumulative incidence of resistant infections up to a given time point might be misleading due to the treatment effect on the terminal event. For instance, an alleged lower resistance rate might be observed for a certain antibiotic treatment, even if all confounders are properly accounted for, simply due to higher death rates under this treatment.

Recently, approaches anchored within the causal inference paradigm have been proposed (Comment et al. 2025, Xu et al. 2020, Nevo & Gorfine 2022, Bühler et al. 2023, Deng et al. 2024). A common theme across this research is the reliance on principal stratification estimands (Frangakis & Rubin 2002). We review several principal stratification approaches

in the context of our motivating study in Section 3. These estimands are based on the notion that within a subset of the population defined by potential event times, causal effects are well-defined. However, as these subsets are typically not identifiable from the observed data, it is crucial to assess whether the subset is meaningful. We contend that these estimands do not conclusively capture the causal effect of interest, as they overlook patients among which a well-defined causal effect exists and, importantly, is of a clinical interest.

Therefore, we focus on a different, previously unexplored, principal stratum: the subpopulation of patients who would have been infected or would have survived within one year after treatment initiation under both antibiotic treatments. The one year mark is chosen based on subject-matter considerations, though other time points can also be considered. We then define the feasible-infection causal effect (FICE) as the causal effect among this subpopulation. We argue that in applications with SCR data, the FICE provides a meaningful causal effect to address questions about the causal effect on the non-terminal event. In the comparison of Access and Watch antibiotics, the FICE is defined among the subpopulation of patients for which the occurrence of a resistant infection is possible under both antibiotic treatments within the specified time period.

We consider two overarching identification approaches for the FICE. First, we develop a partial identification approach in the form of large-sample bounds under new order-preservation (ORP) assumptions. We present bounds under different assumption combinations and discuss the plausibility of these assumptions in our data. As an alternative, we derive FICE identification as a function of an unknown cross-world sensitivity parameter. Namely, we connect the counterfactual event times using a bivariate frailty random variable, where the cross-world parameter is the correlation between the two frailty variables. We consider estimation via an expectation-maximization algorithm (EM) (Dempster et al. 1977), followed by Monte Carlo approximations.

The remainder of the paper is organized as follows. In Section 2, we describe the motivating dataset. In Section 3, we review and compare existing approaches and estimands in the context of studying causal effects of antibiotic usage, and introduce our proposed estimand. In Section 4, we present the two identification approaches and discuss the plausibility of the identification assumptions. In Section 5, we describe the estimation methods for both proposed approaches. In Section 6, we apply our approach to the motivating dataset. In Section 7, we offer concluding remarks.

2 Motivating dataset

The data were obtained from Meir Medical Center, a secondary university-affiliated hospital serving a population of approximately 600,000 people. The dataset included all 38,791 adult patients who had a positive bacterial culture based on samples taken from their blood, urine, sputum, or wounds, between 1 January 2015 and 22 October 2022. Each culture was tested for susceptibility to several antibiotic types, and the dataset included all resistance results.

The dataset contains hospitalization records, including length of stay, antibiotic treatments and culture results, along with demographics and comorbidities, and date of death. We define the *baseline* to be the first instance when a patient received treatment of either amoxicillin-clavulanate or cefuroxime, two commonly prescribed antibiotics in Meir Medical Center, belonging to the Access and Watch classes, respectively. To enhance clarity, we refer to them as *Access* (amoxicillin-clavulanate) and *Watch* (cefuroxime) antibiotics from now on. We remark that the Access and Watch antibiotic groups each contains many more diverse antibiotics, and our comparison is between amoxicillin-clavulanate and cefuroxime only. The treatment as defined in this study is the antibiotic assigned to the patient at baseline. The antibiotic treatment was not randomized and may depend on confounders such as age, medical condition, previous antibiotic usage, and more. Table A1 describes

the distribution of prominent variables among the Watch group (13,959 patients) and the Access group (5,855 patients), categorized by various forms of demographic and clinical information. Patients in the Watch group were generally older; more likely to suffer from several medical conditions, such as dementia and chronic renal failure; and more frequently resided in a residential institution prior to admission. These characteristics of the data align with clinical standards, as physicians tend to prescribe Watch antibiotics to higher-risk patients.

We define the outcome to be time to ceftazidime-resistant infection, up to one year after baseline. We choose ceftazidime as it can be used as a marker for extended-spectrum beta-lactamase, which is a type of antibiotic resistance mechanism with important consequences for hospital infections ([Chowers et al. 2022](#)).

We focus on the one-year mark because the association between antibiotic treatment and resistance decreases over time, and is negligible one year after treatment ([Baraz et al. 2023](#)). A patient is considered to have acquired a resistant infection if he or she had at least one ceftazidime-resistant culture result between five days and one year after baseline treatment.

Within one year after baseline, the unadjusted resistant-infection rates among those treated with Access and Watch antibiotics were 7.3% and 9.9%, respectively. The corresponding unadjusted one-year death rates were 17.2% and 21.9%. At face value, these results might look puzzling, because Watch antibiotics are expected to be more effective in clearing out the bacteria causing the current infection, and consequently should prevent death. However, as discussed above, this is presumably due to confounding, because Watch antibiotics are typically administered to higher-risk patients. After adjusting for potential confounders using a Cox model (Table [A3](#)), the corresponding one-year death rates were 25.2% (CI95%: 23.4%, 26.7%) in the Access group and 19.9% (CI95%: 19.2%, 20.6%) in the Watch group. The resulting estimated risk difference and risk ratio were -5.3% (CI95%: -6.9% , -3.8%)

and 0.79 (CI95%: 0.74, 0.84), respectively.

It should be noted that the positivity assumption may be violated in this dataset. Figure A1 shows the distribution of the estimated *propensity score* (PS), the probability of being treated with the Watch antibiotic conditionally on covariates, among each treatment group. For low estimated PS values, there was almost no overlap between the two PS distributions. To mitigate this issue, we focus on the causal effect among those treated with the Access antibiotic, as in Chowers et al. (2022). To this end, we use matching (Stuart 2010) to adjust for pre-treatment differences in observed covariates between the antibiotic groups. Table A1 presents descriptive statistics within the original and matched datasets. After matching, covariate balance improved substantially, as can be seen from the notable decrease in standardized mean differences between the two antibiotic groups.

Table 1 presents the unadjusted event proportions among the 4,143 matched pairs. Resistant infection rates were relatively similar in the full and matched datasets. In line with the results of the adjusted Cox model in the full dataset, death rates in the matched dataset among the Access antibiotic group were higher than those of the Watch antibiotic group.

To focus on the newly proposed causal estimand and assumptions, we temporarily ignore that the matching implies that the targeted effect is defined among the Access group. We return to this point and describe the matching procedure in Section 6.

3 Setup and causal estimands

3.1 Notations

Let A be the antibiotic treatment, where $A = 0$ corresponds to the Access antibiotic and $A = 1$ to the Watch antibiotic. Using the potential outcomes framework (Rubin 1974), for each unit $i = 1, \dots, n$ in the sample, let $T_{i1}(a)$ and $T_{i2}(a)$ be the potential times to resistant

Table 1: Event proportions in the amoxicillin-clavulanate (Access) and the cefuroxime (Watch) treatment groups within the matched dataset.

	Access	Watch
Sample size	4,143	4,143
Resistant infection	288 (7%)	413 (10.0%)
Infection-free death	746 (18.0%)	616 (14.9%)
Death after infection	113 (2.7%)	147 (3.5%)

infection and death, respectively, had the antibiotic treatment been set to $A = a$. This formulation assumes there is no interference between units (Cox 1958). The units are also assumed to be independent and identically distributed, so we omit the i index when it improves clarity. We set $T_{i1}(a) = \infty$ whenever a resistant infection would not occur within the one year period under treatment level $A = a$.

Let $S_i(a) = \mathbb{1}\{T_{i2}(a) > 1\}$ and $I_i(a) = \mathbb{1}\{T_{i1}(a) \leq 1\}$ be the survival and the resistant bacterial infection indicators, respectively, within one year under treatment level a . Notice that $I_i(a) = 1$ is equivalent to $T_{i1}(a) \leq T_{i2}(a)$. We term the strata $\{i : S_i(0) = 1, S_i(1) = 1\}$, and $\{i : I_i(0) = 1, I_i(1) = 1\}$ the *always-survivors* (*as*) and the *always-infected* (*ai*), respectively, with corresponding population strata proportions π_{as} and π_{ai} . Other subpopulations, defined by post-treatment periods other than one year, might also be considered. For instance, Xu et al. (2020) and Comment et al. (2025) have defined time-varying always-survivors subpopulations. Time-varying subpopulations could be considered in our framework by redefining $S_i(a, r) = \mathbb{1}\{T_{i2}(a) > r\}$, and $I_i(a, r) = \mathbb{1}\{T_{i1}(a) \leq r\}$ and then studying different subpopulations as a function of r . However, as our focus lies in the one-year post-treatment period, we defer the discussion regarding time-varying subpopulations to Appendix B.

3.2 Existing approaches and causal effects

We now review several approaches that have been proposed to address similar problems. First, if we ignore follow-up after resistant infections, our application can be described as a competing risks problem, with the competing events being resistant infection and infection-free death. The total effect $\Pr[T_1(1) \leq t] - \Pr[T_1(0) \leq t]$ (Young et al. 2020) contrasts infection rates between the antibiotic groups, without eliminating the competing event, i.e., death. However, the interpretation and applicability of the total effect can be challenging in practice. Low resistant infection rates under a specific antibiotic treatment might be observed due to high death rates under this treatment. That is, the total effect might quantify changes in infection rates due to mortality differences (Young et al. 2020, Nevo et al. 2021). Yet, the total effect quantifies the possibly meaningful amount of added number of hospitalized patients with a resistant infection resulting from the use of the Watch antibiotic. Hence, it might be useful for resource management, e.g., for determining the number of beds and medical staff capacity in relevant departments. Another possible estimand, the controlled direct effect, contrasts infection rates between two antibiotic treatments under the hypothetical intervention that also prevents the occurrence of death. However, such an intervention remains hypothetical, and is impossible to carry out when the competing event is death, as in our study.

Several authors have utilized principal stratification for SCR data to target causal effects among different subpopulations. One approach generalizes the survivor average causal effect (SACE) (Zhang & Rubin 2003, Ding & Lu 2017, Zehavi & Nevo 2023), the effect among those who would have survived regardless of their treatment. To this end, the SACE can be redefined to target time-to-event outcomes, while also recognizing that the non-terminal event may occur at different times rather than being measured at a single, pre-specified,

time point. In our context, a possible estimand is

$$\text{SACE}(t) = \Pr[T_1(1) \leq t | S(0) = 1, S(1) = 1] - \Pr[T_1(0) \leq t | S(0) = 1, S(1) = 1],$$

for $t \leq 1$. The $\text{SACE}(t)$ compares the resistant infection proportions until time t among the always-survivors. [Xu et al. \(2020\)](#) and [Comment et al. \(2025\)](#) extended the $\text{SACE}(t)$ to acknowledge that the terminal event may also occur at different time points, giving rise to time-varying subpopulations (see [Appendix B](#)).

Recently, [Nevo & Gorfine \(2022\)](#) studied the effect of a specific allele on late-onset Alzheimer’s disease (non-terminal event) and death (terminal event) times. They proposed another family of estimands, based on a different stratification. In terms of our application, this stratification divides the population into four strata according to the order of infection and death times. The always-infected causal effect (AICE) is the causal effect on resistant infection time among the *always-infected* (*ai*), i.e., those who would have had a resistant infection within one year post-treatment, regardless of the antibiotic type. Formally, the $\text{AICE}(t)$ is defined as

$$\text{AICE}(t) = \Pr[T_1(1) \leq t | I(0) = 1, I(1) = 1] - \Pr[T_1(0) \leq t | I(0) = 1, I(1) = 1],$$

for $t \leq 1$. The $\text{AICE}(t)$ might be adequate when the main interest lies in the difference in the non-terminal event proportions, and researchers are unwilling to impose that patients will survive by the end of the study under both treatments. Within the always infected, one could also study the causal effect on the terminal event time ([Nevo & Gorfine 2022](#)).

3.3 Newly proposed estimands

A key issue when discussing effects based on principal or population stratification strategies is the population for which a causal effect is defined. The stratification enables focusing on a well-defined effect, but if the studied stratum excludes certain subpopulations of interest,

this effect might be non-informative. With this in mind, we argue that in our setting, neither the SACE nor the AICE are sufficient to capture causal effects under SCR data. Specifically, in the comparison of Access and Watch antibiotics and their effect on future resistant infection, these estimands exclude from their subpopulation relevant patients.

Define *patient type* (pt) to be an index $pt = 1, \dots, 16$ representing the quadruple $\{I(0), S(0), I(1), S(1)\}$. Table 2 presents all 16 possible pt 's; see also Appendix C for a concrete example of potential event times for each patient type. For example, $pt = 1$ stands for patients who would have died without being infected under both antibiotic treatments, i.e., $\{I(0), S(0), I(1), S(1)\} = \{0, 0, 0, 0\}$.

Both the always-survivors and the always-infected exclude patients who would have had an infection and subsequently died within one year under one antibiotic treatment, while surviving free of infection under the other. In Table 2, those patient types are $pt = 8, 9$. Clearly, there is a clinically-relevant causal effect among these patients, because one antibiotic treatment causes a resistant infection while the other does not. Furthermore, a resistant infection will lead to death for these patient types, highlighting the importance of appropriate treatment for those patients.

Furthermore, the SACE and the AICE are defined among subpopulations that exclude additional relevant patients. Specifically, the always-survivors stratum excludes patient types $pt = 10, 12, 13$. Those patients would have been infected during the one year span under both antibiotics. Hence, a causal effect can be defined among them, even though under at least one antibiotic, they would have died following infection. The always-infected stratum includes those patient types, but excludes patient types $pt = 11, 14, 15$. As these patients would have survived during the one year post-treatment period, a causal effect is well-defined for them.

As a further motivation for studying a larger subpopulation, as targeted by the FICE, recall

Table 2: Subpopulation membership of each patient type (pt), as determined by the values of $\{I(0), S(0), I(1), S(1)\}$. ‘-’ means that the patient type does not belong to any of the subpopulations. ios: infected-or-survivors, ai: always-infected, as: always-survivors. For a detailed discussion regarding the ORP-type assumptions and the monotonicity assumption, see Section 4.1.

pt	I(0)	S(0)	I(1)	S(1)	Subpopulation	Excluded by
1	0	0	0	0	—	
2	1	0	0	0	—	ORP, ios-ORP, weak-ORP
3	0	1	0	0	—	ios-ORP, monotonicity
4	0	0	1	0	—	
5	0	0	0	1	—	
6	1	1	0	0	—	ORP, ios-ORP, weak-ORP monotonicity
7	0	0	1	1	—	
8	1	0	0	1	<i>ios</i>	ORP
9	0	1	1	0	<i>ios</i>	monotonicity
10	1	0	1	0	<i>ai, ios</i>	
11	0	1	0	1	<i>as, ios</i>	
12	1	1	1	0	<i>ai, ios</i>	monotonicity
13	1	0	1	1	<i>ai, ios</i>	
14	1	1	0	1	<i>as, ios</i>	ORP
15	0	1	1	1	<i>as, ios</i>	
16	1	1	1	1	<i>as, ai, ios</i>	

that the one-year ceftazidime-resistant infection rates in the matched data were relatively low, with only 10.0% and 7.0% for patients treated with Watch and Access, respectively. As we show in Section 6, these proportions suggest that the proportion of individuals in the always-infected stratum is low. The SACE does not suffer from this specific problem in the motivating dataset. If, however, mortality rates had been high, then the proportion of the SACE-targeted population would have been low.

To target a more inclusive and relevant subpopulation, we propose to focus on a new principal stratum. For $a = 0, 1$, let $ios(a) = \{i : \{I_i(a) = 1\} \cup \{S_i(a) = 1\}\}$ be the patient subgroup that would have acquired an infection and/or would have survived within one year after antibiotic treatment $A = a$. We propose to focus on the stratum of patients that belong to both $ios(0)$ and $ios(1)$, which we term the *infected-or-survivors* (*ios*). That is, $ios = \{i : i \in ios(0) \cap ios(1)\}$. We also denote π_{ios} for the population proportion of this stratum. As can be seen from Table 2, the *ios* subpopulation is more inclusive than both the always-survivors and the always-infected. It contains all patients that belong to at least one of these strata, and in addition, patient types $pt = 8, 9$ which are neither always-survivors nor always-infected. Looking again at Table 2, we see that the *ios* stratum covers patient types 8–16. A common feature of the excluded patient types is that for at least one antibiotic treatment a , these patients would have died without a resistant infection, that is, $I(a) = S(a) = 0$.

Among the *ios* stratum, we propose a new estimand, the feasible-infection causal effect (FICE), defined by

$$\text{FICE}(t) = \Pr[T_1(1) \leq t \mid ios] - \Pr[T_1(0) \leq t \mid ios],$$

for $t \leq 1$. The $\text{FICE}(t)$ is the resistant infection risk difference by time t in the *ios* stratum. Because infection rates are relatively low, we also consider the analogous risk-ratio scale estimands. For instance, the risk ratio $\text{FICE}(t)$ is defined by $\Pr[T_1(1) \leq$

$t \mid ios] / \Pr[T_1(0) \leq t \mid ios]$. In Appendix B, we discuss causal effects among time-varying subpopulations (Comment et al. 2025, Xu et al. 2020).

3.4 Comparison between the estimands

In this section, we illustrate and compare the characteristics of the various estimands using a synthetic data generating mechanism (DGM). The DGM was based on Markov Cox cause-specific hazard models with patient-level frailty terms for each antibiotic treatment level (Xu et al. 2010, Nevo & Gorfine 2022). Sections 4.2 and 5 provide further information on these models. An additional scenario and the corresponding parameter values for each scenario are given in Appendix D. The parameter values of the scenario presented here were chosen such that infection and mortality rates would roughly reflect the proportions of the events in the motivating dataset.

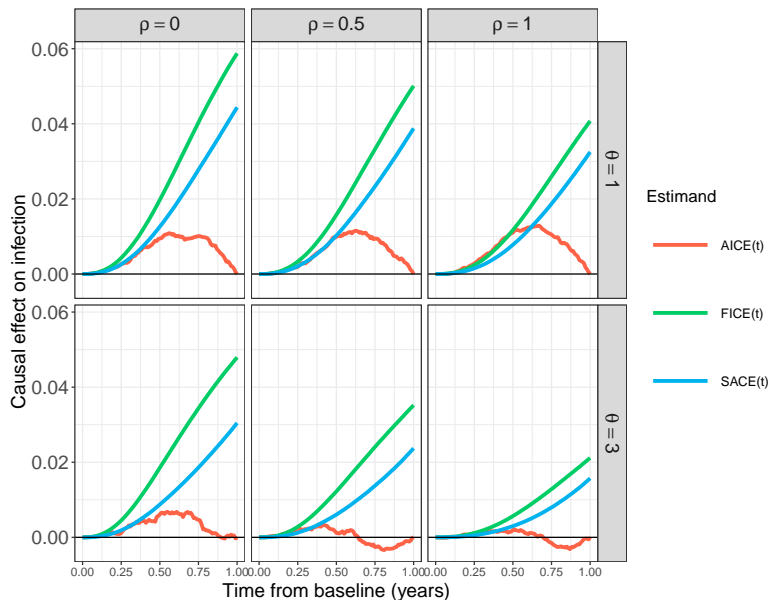
We generated datasets with $n = 30,000,000$, and included one continuous covariate, Weibull baseline hazards, and a bivariate Gamma frailty (random effect) model, with means one, variances θ , and a parameter ρ indicating the correlation between the frailty random effects under each treatment value. Loosely, $\rho = 0$ means that the event times under different treatments are independent (conditionally on covariates) while values away from zero induce cross-world dependence. Large θ values capture within-world dependence between $T_1(a)$ and $T_2(a)$, and may also affect the cross-world dependence, depending on the value of ρ .

Figure 1 compares the FICE(t), the SACE(t) and the AICE(t). We considered several ρ and θ values. As ρ increased, both the FICE(t) and the SACE(t) were smaller for all t values. Further, the estimands varied more with ρ at higher θ values. The trajectories of FICE(t) and SACE(t) over time exhibited similar patterns, both demonstrating monotone increases. In contrast, trends in the AICE(t) diverged from those of the other estimands. At $t = 1$ the value of the AICE(t) is zero as expected, because all patients in the always-infected

stratum experience a resistant infection within one year after treatment.

The similarities in trends and in magnitude between the $FICE(t)$ and the $SACE(t)$, and their distinction from the $AICE(t)$, resulted from the fact the ios stratum contained more always-survivors than always-infected, due to the substantially higher proportion of the former; The always-infected proportion was approximately 1%, whereas the always-survivors proportion ranged from 74% to 80%. The ios proportion exceeded that of always-survivors by roughly 2% – 3%. This phenomenon highlights the pivotal role of strata proportions in shaping the similarity (or the distinction) between the estimands. Consequently, it is essential for researchers to identify and estimate these proportions and to assess membership overlap across strata when examining the behavior of the estimands.

Figure 1: Comparison of different estimands in simulated data over one year following antibiotic treatment.



4 Identification of the FICE

In this section, we describe our two proposed identification approaches. Our first identification approach constructs large-sample bounds for the $FICE(t)$ under relatively weak

assumptions. We compare different types of assumptions and the obtained bounds in Section 4.1. Our second approach, presented in Section 4.2, provides identification up to a sensitivity parameter representing cross-world dependence within a bivariate random effects framework. The results we present in this section can be extended and proven for the more general case of time-varying subpopulations. In Appendix E, we discuss the required adjustments for constructing bounds under the general setup, while identification under the frailty assumptions requires no further adjustments. We also present the results for the risk-ratio scale estimands and all the identification proofs in that appendix.

We assume consistency, so for each patient i , the observed outcomes are $T_{i1} = T_{i1}(A_i)$ and $T_{i2} = T_{i2}(A_i)$. In our dataset, follow-up within the first year after treatment assignment is complete for nearly all patients (censoring rate before the one year mark was approximately 8.5%). We therefore focus on the case of no right censoring, and account for it in the estimation. The identification strategy can be naturally extended to allow for censoring, similarly to Axelrod & Nevo (2023). Let $\tilde{T}_{i1} = \min(T_{i1}, T_{i2}, 1)$ and $\tilde{T}_{i2} = \min(T_{i2}, 1)$ be the observed times, and let $\delta_{i1} = \mathbb{1}\{T_{i1} \leq 1\}$ and $\delta_{i2} = \mathbb{1}\{T_{i2} \leq 1\}$ be indicators for the occurrence of a resistant infection and death, respectively, during follow-up.

When selecting antibiotic treatment, physicians take into account the patient’s clinical status. For instance, patients classified as high-risk are more likely to receive the Watch antibiotic. Therefore, in our motivating problem, we cannot assume that the antibiotic treatment was allocated randomly. We instead leverage the detailed dataset and assume conditional exchangeability (CE), i.e., $A \perp\!\!\!\perp \{T_1(a), T_2(a)\} | \mathbf{X}$, for $a = 0, 1$. Similarly to the identification of the SACE and the AICE, which often requires additional assumptions, consistency and CE do not suffice for FICE identification, and additional assumptions are required.

To summarize, the observed data for each patient i are $(\mathbf{X}_i, A_i, \tilde{T}_{i1}, \delta_{i1}, \tilde{T}_{i2}, \delta_{i2})$. For any

event \mathcal{Q} , let $\Psi_{\mathcal{Q}}(t) = \Pr(\{T_1 \leq t\} \cup \{T_2 > t\} | \mathcal{Q})$ be the conditional probability of being infected by time t , surviving beyond time t , or both. To avoid clutter, we also let $\Psi_{\mathcal{Q}} = \Psi_{\mathcal{Q}}(1)$. For $j = 1, 2$, let $F_{j|\mathcal{Q}}(t) = \Pr(T_j \leq t | \mathcal{Q})$ be the conditional probability of the j -th event (infection or death), occurring before time t . Finally, denote $S_{j|\mathcal{Q}}(t) = 1 - F_{j|\mathcal{Q}}(t)$.

4.1 Bounds under ORP-type assumptions

We start by presenting our partial identification approach, in the form of large-sample bounds for the FICE. To provide motivation for the different assumptions, we revisit our clinical context. Watch antibiotics are aimed at clearing the more severe infections, and consequently, within the same population, they are expected to increase survival probability, compared with Access antibiotics. Concurrently, this major benefit is not necessarily devoid of associated clinical costs, as Watch antibiotics are also more likely to generate future antibiotic resistance, as a result of ecological and evolutionary forces selecting for antibiotic resistant bacteria.

Principal stratum effect identification often relies on monotonicity-type assumptions. In our notation, the monotonicity assumption is $S_i(0) \leq S_i(1)$, for all i . That is, all patients who would have survived beyond one year under the Access antibiotic, would also survive under the Watch antibiotic. Monotonicity within a short time frame, during the hospital stay, might seem plausible; a baseline life-threatening infection cleared by the Access antibiotic would also be cleared when treated with the more aggressive Watch antibiotic. Monotonicity will exclude, for example, individuals of patient type $pt = 3$ (Table 2), which are indeed not expected to be part of the population. Such patients would have survived only under the Access antibiotic ($S(0) = 1, S(1) = 0$), but their death under the Watch antibiotic is not due to a new resistant infection ($I(0) = 0, I(1) = 0$).

However, when considering the wider one-year time window, monotonicity is no longer

plausible, because the Watch antibiotic may lead to a subsequent resistant infection, which may lead to death. This would be the case for $pt = 9$, which belongs to the *ios* stratum. Of note is that for the SACE, monotonicity alone does not imply point identification (Zhang & Rubin 2003, Ding & Lu 2017, Zehavi & Nevo 2023).

Therefore, we consider assumptions of a different nature, that also respect the SCR nature of the data. Our approach extends the approach of Nevo & Gorfine (2022), who considered the following order preservation assumption (ORP).

Assumption 1. *Order-Preservation (ORP).*

$$\forall i : \text{If } I_i(0) = 1, \text{ then } I_i(1) = 1.$$

In our application, ORP implies that the Watch antibiotic cannot prevent a future resistant infection. We focus on bounds under more subtle assumptions for two reasons. First, as previously explained, patients of $pt = 3$ are unlikely to exist in the population, and the ORP assumption does not exclude this patient type. Second, as seen on Table 2, ORP excludes from the population two patient types that belong to the target population ($pt = 8, 14$). Although it seems plausible to assume away the inclusion of these patient types in the population, we prefer to avoid assumptions on the target subpopulation itself.

We introduce a new assumption, which we term the infected or survivors order-preservation assumption (*ios*-ORP).

Assumption 2. *Infected or Survivors Order-Preservation (ios-ORP).*

$$\forall i : \text{If } i \in ios(0), \text{ then } i \in ios(1).$$

Under the *ios*-ORP assumption, every patient that belongs to the *ios*(0) subpopulation, also belongs to the *ios*(1) subpopulation. Namely, any patient who would have been infected or

survived under the Access antibiotic would also have been infected or survived had they received the Watch antibiotic.

As seen in Table 2, the ios-ORP assumption excludes patient types $pt = 2, 3, 6$. The logic behind excluding $pt = 3$ has been previously presented. For $pt = 2, 6$, a future resistant infection occurs under the Access antibiotic treatment, while under the Watch antibiotic these patients would have died without having a resistant infection. Such scenarios are unlikely, because, as previously explained, the Watch antibiotic is more effective against the baseline infection (so death is less likely), but has higher chances of future infection.

The ios-ORP assumption can be falsified by the observed data. Under ios-ORP, $\Pr(\{T_1(0) < 1\} \cup \{T_2(0) > 1\}) \leq \Pr(\{T_1(1) < 1\} \cup \{T_2(1) > 1\})$. Therefore, under CE, we would expect that $E_X[\Psi_{A=0, \mathbf{X}}] \leq E_X[\Psi_{A=1, \mathbf{X}}]$. If this inequality does not hold in the data, then either CE or ios-ORP do not hold.

The next new assumption we introduce is weak-ORP. It is weaker than the two previous assumptions, as shown in Appendix E.

Assumption 3. *Weak Order-Preservation (weak-ORP).*

$$\forall i : \text{If } I_i(0) = 1, \text{ then } i \in \text{ios}(1).$$

Table 2 shows which patient types are excluded by each ORP assumption. Under all three ORP variants, a patient who would have been infected under the Access antibiotic belongs to the *ios* subpopulation. Weak ORP is the weakest assumption (Lemma A2). All patient types excluded under this assumption ($pt = 2, 6$) are also excluded under each of the other two assumptions (separately). Under ios-ORP, $pt = 3$ is also excluded, while under ORP it is not, but $pt = 8, 14$ are excluded. Importantly, the only patient type that is excluded by both weak-ORP and ios-ORP but not under monotonicity is $pt = 2$, which is unlikely to be present in our population of interest. Unlike the ORP assumption, the ios-ORP and

weak-ORP assumptions do not exclude patient types that are part of the *ios* stratum. We establish bounds for the $FICE(t)$ under the latter two ORP-type assumptions. In Appendix E, we also present bounds under consistency and CE only, without imposing any of the ORP assumption.

Starting with ios-ORP, we show in Lemma A4 that under consistency, CE and ios-ORP, the proportion of the *ios* stratum is identified by $\pi_{ios} = E_{\mathbf{X}}[\Psi_{A=0,\mathbf{X}}]$. The proposition below forms $FICE(t)$ bounds under these assumptions.

Proposition 1. *Under consistency, CE and ios-ORP, the $FICE(t)$ is bounded by*

$$\mathcal{L}(t) \leq FICE(t) \leq \mathcal{U}(t),$$

where

$$\begin{aligned} \mathcal{U}(t) &= \min \left\{ 1, \frac{E_{\mathbf{X}}[F_{1|A=1,\mathbf{X}}(t)]}{E_{\mathbf{X}}[\Psi_{A=0,\mathbf{X}}]} \right\} - \frac{E_{\mathbf{X}}[F_{1|A=0,\mathbf{X}}(t)]}{E_{\mathbf{X}}[\Psi_{A=0,\mathbf{X}}]}, \\ \mathcal{L}(t) &= \max \left\{ 0, 1 - \frac{E_{\mathbf{X}}[S_{1|A=1,\mathbf{X}}(t)]}{E_{\mathbf{X}}[\Psi_{A=0,\mathbf{X}}]} \right\} - \frac{E_{\mathbf{X}}[F_{1|A=0,\mathbf{X}}(t)]}{E_{\mathbf{X}}[\Psi_{A=0,\mathbf{X}}]}. \end{aligned}$$

Specifically, under ios-ORP, $\Pr(T_1(0) \leq t | ios)$ is identified by $E_{\mathbf{X}}[F_{1|A=0,\mathbf{X}}(t)]/E_{\mathbf{X}}[\Psi_{A=0,\mathbf{X}}]$, while $\Pr(T_1(1) \leq t | ios)$ is only partially identified. We observe that as π_{ios} (identified by $E_{\mathbf{X}}[\Psi_{A=0,\mathbf{X}}]$) increases, the bounds get tighter. Moreover, if

$$1 - \pi_{ios} < E_{\mathbf{X}}[F_{1|A=1,\mathbf{X}}(t)] < \pi_{ios}, \quad (1)$$

then both of the bounds for $\Pr(T_1(1) \leq t | ios)$ are informative. Condition (1) is satisfied only if $\pi_{ios} > 0.5$. For all t such that (1) holds, the length of the interval $\mathcal{U}(t) - \mathcal{L}(t)$ is constant and equals to $1/\pi_{ios} - 1$.

We now present bounds under the relaxed ORP version, namely, weak-ORP. Under weak-ORP, the *ios* proportion is no longer fully identified. Instead, Lemma A5 provides bounds for π_{ios} under weak-ORP, denoted by $\tilde{\mathcal{U}}_{\pi}$ and $\tilde{\mathcal{L}}_{\pi}$, and use them to derive $FICE(t)$ bounds.

Proposition 2. *Under consistency, CE and weak-ORP, the FICE(t) is bounded by*

$$\tilde{\mathcal{L}}(t) \leq \text{FICE}(t) \leq \tilde{\mathcal{U}}(t),$$

where

$$\tilde{\mathcal{U}}(t) = \frac{\tilde{u}(t)}{1\{\tilde{u}(t) \geq 0\}\tilde{\mathcal{L}}_\pi + 1\{\tilde{u}(t) < 0\}\tilde{\mathcal{U}}_\pi}, \tilde{\mathcal{L}}(t) = \frac{\tilde{l}(t)}{1\{\tilde{l}(t) \geq 0\}\tilde{\mathcal{U}}_\pi + 1\{\tilde{l}(t) < 0\}\tilde{\mathcal{L}}_\pi},$$

and

$$\begin{aligned} \tilde{u}(t) &= \min \left\{ E_{\mathbf{X}}[F_{1|A=1,\mathbf{X}}(t)], E_{\mathbf{X}}[\Psi_{A=0,\mathbf{X}}] \right\} - E_{\mathbf{X}}[F_{1|A=0,\mathbf{X}}(t)], \\ \tilde{l}(t) &= \max \left\{ 0, E_{\mathbf{X}}[\Psi_{A=0,\mathbf{X}}] - E_{\mathbf{X}}[S_{1|A=1,\mathbf{X}}(t)] \right\} - E_{\mathbf{X}}[F_{1|A=0,\mathbf{X}}(t)], \end{aligned}$$

with $1\{\cdot\}$ being the indicator function.

4.2 Identification under frailty assumptions

As an alternative to the partial identification approach detailed above, we also provide a sensitivity analysis for the FICE(t) as a function of a single parameter. Our approach connects two random-effect illness-death models, as originally proposed by [Nevo & Gorfine \(2022\)](#). Each model represents transition probabilities between states $jk \in \{01, 02, 12\}$ for one treatment group, and the models are connected by a bivariate frailty random variable $\boldsymbol{\gamma} = (\gamma_0, \gamma_1)$. The cause-specific hazard functions that define each treatment-specific illness-death model are

$$\lambda_{01}(t|a, \mathbf{X}, \boldsymbol{\gamma}) = \lim_{h \rightarrow 0} \frac{1}{h} \Pr(T_1 \in [t, t+h] | A = a, T_1 \geq t, T_2 \geq t, \mathbf{X}, \boldsymbol{\gamma}), \quad t > 0$$

$$\lambda_{02}(t|a, \mathbf{X}, \boldsymbol{\gamma}) = \lim_{h \rightarrow 0} \frac{1}{h} \Pr(T_2 \in [t, t+h] | A = a, T_1 \geq t, T_2 \geq t, \mathbf{X}, \boldsymbol{\gamma}), \quad t > 0$$

$$\lambda_{12}(t|a, t_1, \mathbf{X}, \boldsymbol{\gamma}) = \lim_{h \rightarrow 0} \frac{1}{h} \Pr(T_2 \in [t, t+h] | A = a, T_1 = t_1, T_2 \geq t, \mathbf{X}, \boldsymbol{\gamma}), \quad t > t_1 > 0.$$

for $a = 0, 1$.

The following frailty assumptions establish the connection between the distributions of the potential event times through the frailty γ , where an unidentifiable parameter, denoted as ρ , governs the cross-world correlation.

Assumption 4. *There exists a bivariate random variable $\gamma = (\gamma_0, \gamma_1)$, fulfilling the following conditions:*

(i) $A \perp\!\!\!\perp \{T_1(a), T_2(a), \gamma_a\} | \mathbf{X}$, for $a = 0, 1$.

(ii) *Given \mathbf{X} and γ , the joint distribution of the potential event times can be separated into the following components*

$$f(T_1(0), T_2(0), T_1(1), T_2(1) | \mathbf{X}, \gamma_0, \gamma_1) = f(T_1(0), T_2(0) | \mathbf{X}, \gamma_0) f(T_1(1), T_2(1) | \mathbf{X}, \gamma_1),$$

where $f(\cdot)$ is a density function.

(iii) $\gamma \perp\!\!\!\perp \mathbf{X}$. *In words, the frailty variable γ and the covariates \mathbf{X} are independent.*

(iv) *The hazard function has the following multiplicative form: $\lambda_{jk}(t|a, \mathbf{X}, \gamma) = \gamma_a \lambda'_{jk}(t|a, \mathbf{X})$ for $j = 0, k = 1, 2$, and $\lambda_{12}(t|t_1, a, \mathbf{X}, \gamma) = \gamma_a \lambda'_{12}(t|t_1, a, \mathbf{X})$, for $a = 0, 1$ and for some functions λ'_{jk} .*

(v) *The probability density function of γ , termed $f_{\theta}(\gamma)$, is known up to the parameters θ , and the parameters(s) that govern $f_{\theta}(\gamma)$ are identifiable from the observed data.*

Part (i) is similar to the CE assumption, where γ_a is also included together with the potential event times. Part (ii) asserts that conditionally on the covariates \mathbf{X} and the frailty γ , the cross-world event time pairs are independent, and that conditionally on the frailty γ_a and covariates \mathbf{X} , potential event times under treatment a are independent of γ_{1-a} . Parts (iv) and (v) pertain to the identification of the observed data distribution (for $T_1 < T_2$) and of $f_{\theta}(\gamma)$.

The proposition below provides the identification of the FICE(t) and of the *ios* stratum

proportion, as a function of the unidentifiable parameter ρ , under the frailty assumptions.

Proposition 3. *Under consistency and the frailty assumptions (Assumption 4), the FICE is identified from the observed data by*

$$FICE(t) = \frac{1}{\pi_{ios}(\boldsymbol{\theta}, \rho)} \left\{ E_{\mathbf{X}} \left[E_{\gamma} \left[F_{1|A=1, \mathbf{X}, \gamma_1}(t) \Psi_{A=0, \mathbf{X}, \gamma_0} - F_{1|A=0, \mathbf{X}, \gamma_0}(t) \Psi_{A=1, \mathbf{X}, \gamma_1} \right] \right] \right\},$$

where $\pi_{ios}(\boldsymbol{\theta}, \rho) = E_{\mathbf{X}} \left\{ E_{\gamma} [\Psi_{A=0, \mathbf{X}, \gamma_0} \Psi_{A=1, \mathbf{X}, \gamma_1}] \right\}$ is the proportion of the ios stratum in the population under the frailty assumptions.

Monte Carlo simulations can be used to approximate these expectations. The SACE(t) can be identified under the frailty assumptions as well.

In our data analysis in Section 6, we assume that for $a = 0, 1$, γ_a is a Gamma frailty variable, with a shape parameter θ_a^{-1} and a scale parameter θ_a . The vector $\boldsymbol{\gamma}$ is then a bivariate Gamma variable, with means one, variances θ_0 and θ_1 , and the sensitivity parameter ρ is the correlation between γ_0 and γ_1 . More generally, researchers can also specify other probability distributions for $\boldsymbol{\gamma}$.

5 Semi-parametric model and estimation

Calculating the large-sample bounds entails estimation of $F_{1|A=a, \mathbf{X}}(t)$ and $\boldsymbol{\psi}_{A=a, \mathbf{X}}(t)$, for both $a = 0, 1$. This could be done using any regression-based illness-death model. Frailty random variables can be used to model dependence between $T_1(a)$ and $T_2(a)$, without modeling cross-world independence. We describe one such approach at the end of this section.

For estimation of and inference about the FICE(t) under the frailty assumptions, we will

use the following hazard models.

$$\begin{aligned}\lambda_{01}(t|a, \mathbf{X}, \gamma) &= \gamma_a \lambda_{01}^0(t|a) \exp(\mathbf{X}^t \boldsymbol{\beta}_{01}^a), \quad t > 0 \\ \lambda_{02}(t|a, \mathbf{X}, \gamma) &= \gamma_a \lambda_{02}^0(t|a) \exp(\mathbf{X}^t \boldsymbol{\beta}_{02}^a), \quad t > 0\end{aligned}\tag{2}$$

$$\lambda_{12}(t|t_1, a, \mathbf{X}, \gamma) = \gamma_a \lambda_{12}^0(t|a) \exp(\mathbf{X}^t \boldsymbol{\beta}_{12}^a), \quad t > t_1 > 0,$$

with unspecified baseline hazard functions $\lambda_{jk}^0(t|a)$. Denote the cumulative baseline hazard functions as $\Lambda_{jk}^0(t|a) = \int_0^t \lambda_{jk}^0(u|a) du$. We define the following quantities: $\tilde{\boldsymbol{\theta}} = (\theta_0, \theta_1)$, $\tilde{\boldsymbol{\beta}} = (\boldsymbol{\beta}^0, \boldsymbol{\beta}^1)$, $\tilde{\boldsymbol{\lambda}}_0(t) = (\boldsymbol{\lambda}^0(t), \boldsymbol{\lambda}^1(t))$, and $\tilde{\boldsymbol{\Lambda}}_0(t) = (\boldsymbol{\Lambda}^0(t), \boldsymbol{\Lambda}^1(t))$, where, for $a = 0, 1$, $\boldsymbol{\beta}^a = (\boldsymbol{\beta}_{01}^a, \boldsymbol{\beta}_{02}^a, \boldsymbol{\beta}_{12}^a)$, $\boldsymbol{\lambda}^a(t) = (\lambda_{01}^0(t|a), \lambda_{02}^0(t|a), \lambda_{12}^0(t|a))$, and $\boldsymbol{\Lambda}^a(t) = (\Lambda_{01}^0(t|a), \Lambda_{02}^0(t|a), \Lambda_{12}^0(t|a))$. Define also

$$\begin{aligned}k_i &= H_{01}^0(\tilde{T}_{i1}|a_i) \exp(\mathbf{X}_i^t \boldsymbol{\beta}_{01}^{a_i}) + H_{02}^0(\tilde{T}_{i1}|a_i) \exp(\mathbf{X}_i^t \boldsymbol{\beta}_{02}^{a_i}) \\ &\quad + [H_{12}^0(\tilde{T}_{i2}|a_i) - H_{12}^0(\tilde{T}_{i1}|a_i)] \exp(\mathbf{X}_i^t \boldsymbol{\beta}_{12}^{a_i}) \delta_{i1}.\end{aligned}$$

In Appendix F we show that the likelihood function, integrated over the frailty distribution, is equal to

$$\begin{aligned}L(\tilde{\boldsymbol{\theta}}, \tilde{\boldsymbol{\Lambda}}_0, \tilde{\boldsymbol{\lambda}}_0, \tilde{\boldsymbol{\beta}}) &= \prod_{i=1}^n \left\{ [\lambda_{01}^0(\tilde{T}_{i1}|a)]^{\delta_{i1}} [\lambda_{02}^0(\tilde{T}_{i1}|a)]^{(1-\delta_{i1})\delta_{i2}} [\lambda_{12}^0(\tilde{T}_{i2}|a)]^{\delta_{i1}\delta_{i2}} \right. \\ &\quad \left. \exp\left(\delta_{i1} X_i^t \boldsymbol{\beta}_{01}^{A_i} + (1-\delta_{i1})\delta_{i2} X_i^t \boldsymbol{\beta}_{02}^{A_i} + \delta_{i1}\delta_{i2} X_i^t \boldsymbol{\beta}_{12}^{A_i}\right) (-1)^{\delta_{i1}+\delta_{i2}} \phi_{a_i}^{(\delta_{i1}+\delta_{i2})}(k_i) \right\},\end{aligned}$$

where for $a = 0, 1$, $q = 0, 1, 2$, the function $\phi_a^{(q)}(k)$ is the q -th derivative of $E[\exp(-k\gamma_a)]$ with respect to k .

Estimation of the parameters can be achieved by employing an EM algorithm (Dempster et al. 1977), described in Appendix F. After parameter estimation, we use Monte Carlo simulations to estimate the quantities in the identification result from Proposition 3. Standard errors (SEs) and confidence intervals (CIs) can be estimated using a bootstrap procedure.

Bounds estimation can be based on the same models, while ignoring the correlation parameter ρ as the quantities that establish the bounds do not involve any cross-world terms.

Importantly, in this approach, the frailty random variables are used only for estimation purposes, not identification.

6 Application to the motivating example

We applied our two identification approaches to quantify the causal effect of using a cefuroxime, a Watch antibiotic treatment, compared with amoxicillin-clavulanate, an Access antibiotic treatment, on future ceftazidime-resistant infection. As discussed in Section 2, we first matched each patient in the Access group to a single patient in the Watch group, without replacement. Matching was based on the Mahalanobis distance with a *caliper* (Rubin & Thomas 2000, Stuart 2010) of 0.3 standard deviations on the estimated PS. Both the Mahalanobis distance and the PS model (Section A) included all covariates described in Table A1. Due to the difference in the estimated PS distributions between the two antibiotic groups, only 4,143 out of the 5,855 (71%) patients who received Access antibiotic had a satisfactory match. However, the results did not change substantially when a larger caliper was taken or when matching was done solely on the estimated PS. Due to the matching, the causal effects we study cover the population of patients who are treated with Access antibiotic.

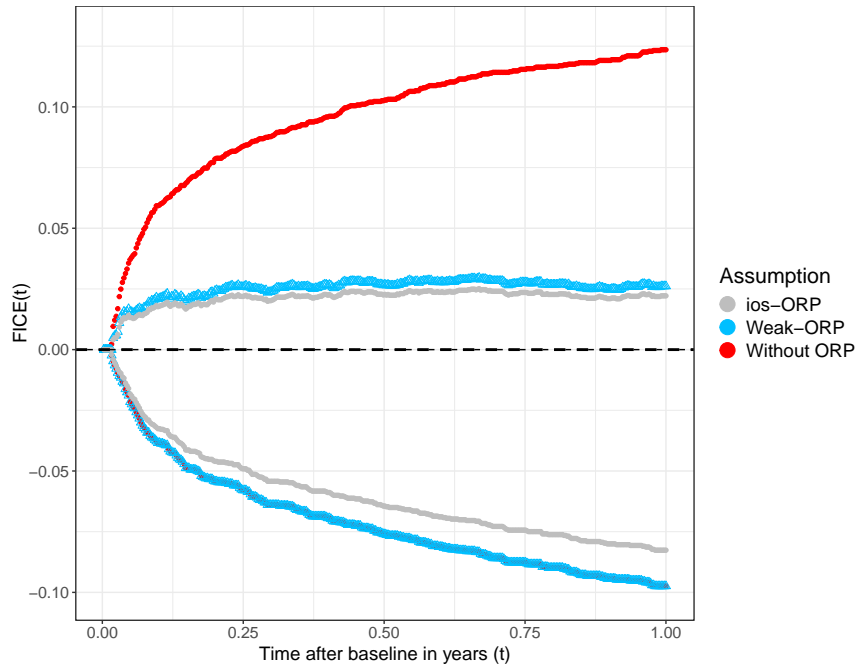
SEs were estimated by a pair-level Bootstrap with 200 repetitions. Wald-type 95% confidence intervals were then calculated.

Starting with the large-sample bounds, the quantities needed for calculating the bounds were estimated by two frailty illness-death models, estimated separately at each treatment group by the EM algorithm (Appendix F). Let $\hat{E}_{\mathbf{X}}(\cdot)$ be the empirical mean over the distribution of \mathbf{X} in the matched dataset. The estimated mean Ψ 's were $\hat{E}_{\mathbf{X}}[\hat{\Psi}_{A=0,\mathbf{X}}] = 0.815$ and $\hat{E}_{\mathbf{X}}[\hat{\Psi}_{A=1,\mathbf{X}}] = 0.876$. Because $\hat{E}_{\mathbf{X}}[\hat{\Psi}_{A=0,\mathbf{X}}] < \hat{E}_{\mathbf{X}}[\hat{\Psi}_{A=1,\mathbf{X}}]$, the ios-ORP assumption was not falsified by our data. The estimated ios stratum proportion under ios-ORP was

81.5% (CI95%: 80.5%, 82.4%). The bounds for π_{ios} under weak-ORP and without ORP assumptions were identical (Appendix E) and estimated to be [69.1%, 81.5%].

Figure 2 presents the estimated FICE(t) bounds. On the difference scale, the one-year estimated FICE bounds without ORP assumptions, under weak-ORP, and under ios-ORP were $[-9.7\%, 12.4\%]$, $[-9.7\%, 2.6\%]$ and $[-8.3\%, 2.2\%]$, respectively. As one may expect, the stronger the assumption taken, the narrower the bounds became. After approximately 90 days ($t \approx 0.25$), the upper bounds under the ORP assumptions did not vary considerably. On the risk-ratio scale (Figure A4), the bounds under weak-ORP and ios-ORP coincide analytically (see Appendix E). The upper bound under weak-ORP decreased from approximately 2.00 two weeks after baseline to 1.27 (CI95%: 1.07, 1.46) after one year, and the lower bound was zero for all t , i.e., it was not informative. The estimated bounds without ORP-type assumptions were also not informative.

Figure 2: Estimated bounds for the FICE(t) on the difference-scale without ORP-type assumptions (without ORP), and under weak-ORP and ios-ORP. The lower bound without ORP assumptions was the same as the one under weak-ORP.



Turning to the alternative sensitivity analysis under the frailty assumptions, we employed the EM algorithm for the illness-death models with bivariate Gamma frailty distribution with varying $\rho = \text{Corr}(\gamma_0, \gamma_1)$ values. The obtained estimates were relatively robust to different ρ values. Therefore, we present here the results for $\rho = 0$, and compare the results for other ρ values in Appendix G. The estimated values of θ_0 and θ_1 were 1.78 (CI95%: 1.17, 2.52) and 0.89 (CI95%: 0.33, 1.42), respectively. The ios proportion was estimated to be 4.5% larger than the always-survivors proportion. These estimated proportions were $\hat{\pi}_{ios} = 74.0\%$ (CI95%: 72.9%, 75.2%) and $\hat{\pi}_{as} = 69.5\%$ (CI95%: 68.4%, 70.7%). Due to the overlap between these subpopulations, the estimated effects within the two strata did not differ substantially. The estimated always-infected proportion was notably low ($\hat{\pi}_{ai} = 0.9\%$) and we therefore do not present results for the AICE.

Figure 3: Comparison between estimates of the different estimands within one year after baseline under the frailty assumptions with $\rho = 0$. The upper panel shows the various estimates on the difference scale. The lower panel shows the various estimates on the risk-ratio scale.

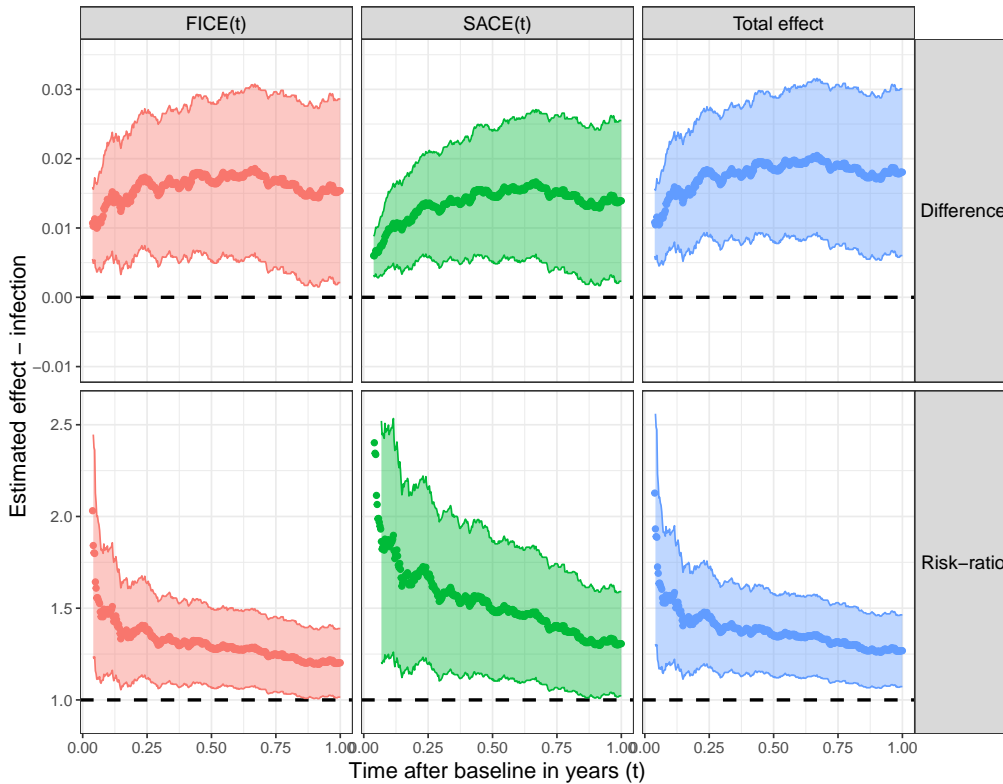


Figure 3 depicts estimated causal effects for $t \leq 1$ along with the 95% confidence intervals. At $t = 1$, the FICE(t) and the SACE(t) were estimated to be 1.5% (CI95%: 0.2%, 2.9%) and 1.4% (CI95%: 0.2%, 2.6%), respectively. The estimated total effect at $t = 1$ was 1.8% (CI95%: 0.6%, 3.0%). The total effect was about 20% larger than the FICE and the SACE, as the Watch antibiotic presumably prevents death, resulting in higher infection rates under the Watch antibiotic. This finding illustrates the subtlety when interpreting the total effect. The proportion of the two patient types that would have been infected and subsequently died under one antibiotic treatment but not under the other ($pt = 8, 9$) was 3.9% (CI95%: 3.4%, 4.3%). The effect among them was relatively high, although not significant, amounting to 4.4% (CI95%: -8.7%, 17.5%), highlighting the necessity of including them within the population of interest. As discussed in Section 3.3, the FICE does include them, while the SACE and the AICE do not.

Moving to the risk-ratio scale, the FICE, the SACE and the total effect decreased with time from approximately 2.00 after the first two weeks to 1.20 (CI95%: 1.02, 1.39), 1.31 (CI95%: 1.02%, 1.59%) and 1.27 (CI95%: 1.07%, 1.46%), respectively, during the one-year period.

In summary, while the large-sample bounds are more informative under ORP assumptions than the bounds without ORP assumptions, they do not reject the option of a null result. In contrast, our frailty-based analysis reveals that a causal effect of using Watch instead of Access on future ceftazidime-resistant infection exists. The estimated number needed to harm was approximately 65 (CI95%: 35, 472). This means that for every 10,000 ios patients treated with the Access antibiotic, had we replaced it with the Watch antibiotic, we would expect about 150 more patients to acquire a resistant infection. The estimated ios proportion was high under both the ORP-type assumptions and the frailty assumptions. This indicates that this subpopulation is highly relevant and that targeting the FICE achieves our original motivation of capturing effects in a large subpopulation.

7 Discussion

In this paper, we proposed a principal stratification approach to study the causal effect on the non-terminal event time in SCR settings. Our proposed estimand, the $FICE(t)$, is defined in a new stratum among which a well-defined causal effect exists and is informative. This stratum is more inclusive than previously-proposed subpopulations. We derive $FICE(t)$ bounds under new ORP assumptions, and provide a principal-stratification oriented examination of the plausibility of these assumptions. As an alternative strategy, we conduct a sensitivity analysis that incorporates a frailty random variable, resembling the approaches of [Xu et al. \(2020\)](#) and [Nevo & Gorfine \(2022\)](#).

Our approach offers broad applicability to researchers in a variety of disciplines. One particularly urgent, yet understudied, public-health problem to which it can be applied to is quantifying the causal effect of antibiotic usage on subsequent antibiotic resistance. To demonstrate its utility, we apply the proposed method to our motivating dataset, estimating the excess ceftazidime-resistance burden from Watch versus Access use. While in this application the focus was on the non-terminal event, causal effects on the terminal event within strata covered in this paper can also be targeted.

Several avenues remain for future research. First, extending the framework to handle repeated or time-varying antibiotic use. Second, developing full identification strategies for causal effects on the non-terminal event time under alternative assumptions. Specifically, assumptions whose violations can be captured by a sensitivity parameter, similarly to the approaches adopted by [Ding & Lu \(2017\)](#) and [Zehavi & Nevo \(2023\)](#) for SACE identification. While our methodology was tailored to address the causal effect of antibiotic usage on future antibiotic resistance, we believe it may also constitute a step toward strengthening principal stratification tools for studying causal effects in SCR settings more broadly.

8 Data Availability Statement

The code for the numerical example and illustrative analysis of the synthetic data is available at <https://github.com/TamirZe/SCR-antibiotics>.

References

- Axelrod, R. & Nevo, D. (2023), ‘A sensitivity analysis approach for the causal hazard ratio in randomized and observational studies’, *Biometrics* **79**(3), 2743–2756.
- Baraz, A., Chowers, M., Nevo, D. & Obolski, U. (2023), ‘The time-varying association between previous antibiotic use and antibiotic resistance’, *Clinical Microbiology and Infection* **29**(3), 390–e1.
- Bell, B. G., Schellevis, F., Stobberingh, E., Goossens, H. & Pringle, M. (2014), ‘A systematic review and meta-analysis of the effects of antibiotic consumption on antibiotic resistance’, *BMC infectious diseases* **14**(1), 1–25.
- Bühler, A., Cook, R. J. & Lawless, J. F. (2023), ‘Multistate models as a framework for estimand specification in clinical trials of complex processes’, *Statistics in Medicine* **42**(9), 1368–1397.
- Chowers, M., Zehavi, T., Gottesman, B. S., Baraz, A., Nevo, D. & Obolski, U. (2022), ‘Estimating the impact of cefuroxime versus cefazolin and amoxicillin/clavulanate use on future collateral resistance: a retrospective comparison’, *Journal of Antimicrobial Chemotherapy* **77**(7), 1992–1995.
- Comment, L., Mealli, F., Haneuse, S. & Zigler, C. M. (2025), ‘Survivor average causal effects for continuous time: A principal stratification approach to causal inference with semicompeting risks’, *Biometrical Journal* **67**(2), e70041.

- Cox, D. R. (1958), ‘Planning of experiments.’
- Dempster, A. P., Laird, N. M. & Rubin, D. B. (1977), ‘Maximum likelihood from incomplete data via the em algorithm’, *Journal of the Royal Statistical Society: Series B (Methodological)* **39**(1), 1–22.
- Deng, Y., Wang, Y. & Zhou, X.-H. (2024), ‘Direct and indirect treatment effects in the presence of semicompeting risks’, *Biometrics* **80**(2), ujae032.
- Ding, P. & Lu, J. (2017), ‘Principal stratification analysis using principal scores’, *Journal of the Royal Statistical Society: Series B (Statistical Methodology)* **79**(3), 757–777.
- Fix, E. & Neyman, J. (1951), ‘A simple stochastic model of recovery, relapse, death and loss of patients’, *Human Biology* **23**(3), 205–241.
- Frangakis, C. E. & Rubin, D. B. (2002), ‘Principal stratification in causal inference’, *Biometrics* **58**(1), 21–29.
- Gladstone, R. A., McNally, A., Pöntinen, A. K., Tonkin-Hill, G., Lees, J. A., Skytén, K., Cléon, F., Christensen, M. O., Haldorsen, B. C., Bye, K. K. et al. (2021), ‘Emergence and dissemination of antimicrobial resistance in escherichia coli causing bloodstream infections in norway in 2002–17: a nationwide, longitudinal, microbial population genomic study’, *The Lancet Microbe* **2**(7), e331–e341.
- Gorfine, M., Keret, N., Ben Arie, A., Zucker, D. & Hsu, L. (2021), ‘Marginalized frailty-based illness-death model: application to the UK-Biobank survival data’, *Journal of the American Statistical Association* **116**(535), 1155–1167.
- Hsieh, J.-J. & Huang, Y.-T. (2012), ‘Regression analysis based on conditional likelihood approach under semi-competing risks data’, *Lifetime data analysis* **18**, 302–320.

- Kats, L. & Gorfine, M. (2023), ‘An accelerated failure time regression model for illness–death data: A frailty approach’, *Biometrics* **79**(4), 3066–3081.
- Lee, K. H., Haneuse, S., Schrag, D. & Dominici, F. (2015), ‘Bayesian semiparametric analysis of semicompeting risks data: investigating hospital readmission after a pancreatic cancer diagnosis’, *Journal of the Royal Statistical Society Series C: Applied Statistics* **64**(2), 253–273.
- Murray, C. J., Ikuta, K. S., Sharara, F., Swetschinski, L., Aguilar, G. R., Gray, A., Han, C., Bisignano, C., Rao, P., Wool, E. et al. (2022), ‘Global burden of bacterial antimicrobial resistance in 2019: a systematic analysis’, *The lancet* **399**(10325), 629–655.
- Nevo, D., Blacker, D., Larson, E. B. & Haneuse, S. (2022), ‘Modeling semi-competing risks data as a longitudinal bivariate process’, *Biometrics* **78**(3), 922–936.
- Nevo, D. & Gorfine, M. (2022), ‘Causal inference for semi-competing risks data’, *Biostatistics* **23**(4), 1115–1132.
- Nevo, D., Ogino, S. & Wang, M. (2021), ‘Reflection on modern methods: causal inference considerations for heterogeneous disease etiology’, *International Journal of Epidemiology* **50**(3), 1030–1037.
- Okeke, I. N., de Kraker, M. E., Van Boeckel, T. P., Kumar, C. K., Schmitt, H., Gales, A. C., Bertagnolio, S., Sharland, M. & Laxminarayan, R. (2024), ‘The scope of the antimicrobial resistance challenge’, *The Lancet* **403**(10442), 2426–2438.
- Peng, L. & Fine, J. P. (2007), ‘Regression modeling of semicompeting risks data’, *Biometrics* **63**(1), 96–108.
- Rubin, D. B. (1974), ‘Estimating causal effects of treatments in randomized and nonrandomized studies.’, *Journal of educational Psychology* **66**(5), 688.

- Rubin, D. B. & Thomas, N. (2000), ‘Combining propensity score matching with additional adjustments for prognostic covariates’, *Journal of the American Statistical Association* **95**(450), 573–585.
- Saciuk, Y., Nevo, D., Chowers, M. & Obolski, U. (2025), ‘Penicillin allergy as an instrumental variable for estimating antibiotic effects on resistance’, *Nature Communications* **16**(1), 1088.
- Stuart, E. A. (2010), ‘Matching methods for causal inference: A review and a look forward’, *Statistical science* **25**(1), 1.
- Tong, J., Kahan, B., Harhay, M. O. & Li, F. (2025), ‘Semiparametric principal stratification analysis beyond monotonicity’, *arXiv preprint arXiv:2501.17514* .
- Ventola, C. L. (2015), ‘The antibiotic resistance crisis: part 1: causes and threats’, *Pharmacy and therapeutics* **40**(4), 277.
- WHO (2017), ‘The Selection and Use of Essential Medicines’: Report of the WHO Expert Committee, 2017 (Including the 20th WHO Model List of Essential Medicines and the 6th Model List of Essential Medicines for Children)’.
- Xu, J., Kalbfleisch, J. D. & Tai, B. (2010), ‘Statistical analysis of illness–death processes and semicompeting risks data’, *Biometrics* **66**(3), 716–725.
- Xu, Y., Scharfstein, D., Müller, P. & Daniels, M. (2020), ‘A Bayesian nonparametric approach for evaluating the causal effect of treatment in randomized trials with semi-competing risks’, *Biostatistics* .
- Young, J. G., Stensrud, M. J., Tchetgen Tchetgen, E. J. & Hernán, M. A. (2020), ‘A causal framework for classical statistical estimands in failure-time settings with competing events’, *Statistics in Medicine* **39**(8), 1199–1236.

- Zehavi, T. & Nevo, D. (2023), ‘Matching methods for truncation by death problems’, *Journal of the Royal Statistical Society Series A: Statistics in Society* **186**(4), 659–681.
- Zhang, J. L. & Rubin, D. B. (2003), ‘Estimation of causal effects via principal stratification when some outcomes are truncated by “death”’, *Journal of Educational and Behavioral Statistics* **28**(4), 353–368.

Appendix

A Additional information about the motivating dataset

In this section, we provide information about key variables in the original motivating and matched datasets, and provide the results of the models mentioned in Section 2.

We begin with Table A1, which presents the distribution of the set of covariates \mathbf{X} among the Watch group (13,959 patients in the full dataset, 4,143 patients in the matched dataset) and the Access group (5,855 and 4,183 patients), categorized by various forms of demographic and clinical information. As discussed in Section 2, patients in the Watch group were generally older; more likely to suffer from several medical conditions, such as dementia and chronic renal failure; and more frequently resided in a residential institution prior to admission. These patterns are expected and align with clinical practice, as the Watch antibiotic is often prescribed to high-risk patients.

Table A1: Covariates distribution in the full and matched datasets. Matching was on the Mahalanobis distance with a caliper on the estimated propensity score ($c = 0.3$ standard deviation of the estimated propensity score). For discrete covariates, frequencies (proportions) are reported. For the covariate age, the mean (standard deviation) is reported. SMD: standardized mean difference. CRF: chronic renal failure. Cefta: ceftazidime.

	Full dataset			Matched dataset		
	Access	Watch	SMD	Access	Watch	SMD
N	5,855	13,959		4,143	4,143	
Demographics						
Age	56.0 (25.2)	69.0 (22.0)	0.55	57.9 (26.4)	61.2 (24.3)	0.13
Male [†]	3041 (51.9%)	7668 (54.9%)	0.06	2192 (52.9%)	2195 (53%)	0.00
Sample location at baseline						
Other	454 (7.8%)	482 (3.5%)	0.19	306 (7.4%)	262 (6.3%)	0.04
Not taken	3,093 (52.8%)	7,217 (51.7%)	0.02	2481 (59.9%)	2465 (59.5%)	0.01
Multiple sources	390 (6.7%)	1,281 (9.2%)	0.09	320 (7.7%)	302 (7.3%)	0.02
Urine	562 (9.6%)	3,584 (25.7%)	0.43	551 (13.3%)	580 (14%)	0.02
Wound	1,016 (17.3%)	217 (1.5%)	0.56	196 (4.7%)	216 (5.2%)	0.02
Blood	182 (3.1%)	930 (6.7%)	0.17	167 (4%)	169 (4.1%)	0.00
Sputum	158 (2.7%)	248 (1.8%)	0.06	122 (2.9%)	149 (3.6%)	0.04
Arrived from						
Other	1,074 (18.3%)	1,441 (10.3%)	0.23	762 (18.4%)	691 (16.7%)	0.04
Home	4,098 (70%)	10,310 (73.9%)	0.09	2,784 (67.2%)	2,837 (68.5%)	0.03
Institution	683 (11.7%)	2,208 (15.8%)	0.12	597 (14.4%)	615 (14.8%)	0.01
Hospitalization unit						
Other	2,445 (41.8%)	1,500 (10.7%)	0.75	1,096 (26.5%)	1,018 (24.6%)	0.04
Internal	1,839 (31.4%)	8,883 (63.6%)	0.68	1,767 (42.6%)	1,820 (43.9%)	0.03
Surgical	1,571 (26.8%)	3,576 (25.6%)	0.03	1,280 (30.9%)	1,305 (31.5%)	0.01
Medical history						
Dementia	313 (5.3%)	1,252 (9%)	0.14	283 (6.8%)	295 (7.1%)	0.01
CRF	452 (7.7%)	1,604 (11.5%)	0.13	341 (8.2%)	348 (8.4%)	0.01
Immunosuppression	414 (7.1%)	1,370 (9.8%)	0.10	345 (8.3%)	370 (8.9%)	0.02
Diabetes	1,375 (23.5%)	3,352 (24%)	0.01	856 (20.7%)	866 (20.9%)	0.01
Catheter	631 (10.8%)	3,123 (22.4%)	0.32	571 (13.8%)	609 (14.7%)	0.03
Previous antibiotic use	1,000 (17.1%)	2,049 (14.7%)	0.07	699 (16.9%)	729 (17.6%)	0.02
Previous cefta culture (365 days) [†]	719 (12.4%)	1,401 (10.1%)	0.07	539 (13%)	541 (13.1%)	0.00
Medical information						
Arrival to culture (> 2 days) [†]	2,317 (39.6%)	6,016 (43.1%)	0.07	1,850 (44.6%)	1,876 (45.3%)	0.01
Arrival to treatment (> 2 days) [†]	1,041 (17.8%)	3,114 (22.3%)	0.11	806 (19.4%)	835 (20.1%)	0.02

[†] Male is an indicator variable denoting whether the patient is a male. Arrival to culture and Arrival to treatment are indicators for whether arrival preceded culture collection or antibiotic treatment initiation, respectively, by more than two days. Previous ceftazidime culture is an indicator variable denoting whether a ceftazidime culture was taken before baseline.

We now present the results from the models we employed in Section 2 for data description. All models were estimated using the same set of covariates, as in the main analysis. Table A2 shows the hazard ratio estimates obtained by the Cox regression model for time to death, ignoring infection status, where the observed data were \tilde{T}_2 , δ_2 , and \mathbf{X} . Estimated 95% Wald-type confidence intervals are also reported. We estimated the propensity score via a logistic regression model. Table A3 shows the odds ratios estimates along with their estimated 95% Wald-type confidence intervals. Figure A1 depicts the estimated propensity score distributions by antibiotic groups.

Table A2: Cox model for time-to-death analysis ignoring infection times. HR: hazard ratio; CI95%: 95% confidence intervals. Cefta: ceftazidime.

Covariate	HR	CI95%
Access ($A = 0$)	1.00	
Watch ($A = 1$)	0.73	[0.68, 0.79]
Demographics		
Age	1.23	[1.14, 1.33]
Age ²	0.998	[0.997, 0.999]
Age ³	1.00	[1.00, 1.00]
Male [†]	0.89	[0.83, 0.95]
Sample location at baseline		
Other	1.00	
Not taken	0.68	[0.57, 0.81]
Multiple sources	0.87	[0.72, 1.04]
Urine	0.64	[0.54, 0.77]
Wound	0.50	[0.38, 0.64]
Blood	0.99	[0.81, 1.20]
Sputum	0.76	[0.58, 0.99]
Arrived from		
Other	1.00	
Home	0.87	[0.76, 0.99]
Institution	1.28	[1.11, 1.48]
Hospitalization unit		
Other	1.00	
Internal	1.23	[1.09, 1.39]
Surgical	0.58	[0.50, 0.66]
Medical history		
Dementia	0.89	[0.81, 0.98]
CRF	1.06	[0.97, 1.16]
Immunosuppression	1.49	[1.36, 1.63]
Diabetes	1.04	[0.97, 1.11]
Catheter	1.79	[1.67, 1.91]
Previous antibiotic (any)	1.32	[1.22, 1.43]
Previous cefta culture (365 days) [†]	1.35	[1.22, 1.49]
Medical information		
Arrival to culture (>2 days) [†]	0.98	[0.90, 1.06]
Arrival to treatment (>2 days) [†]	1.07	[0.99, 1.16]

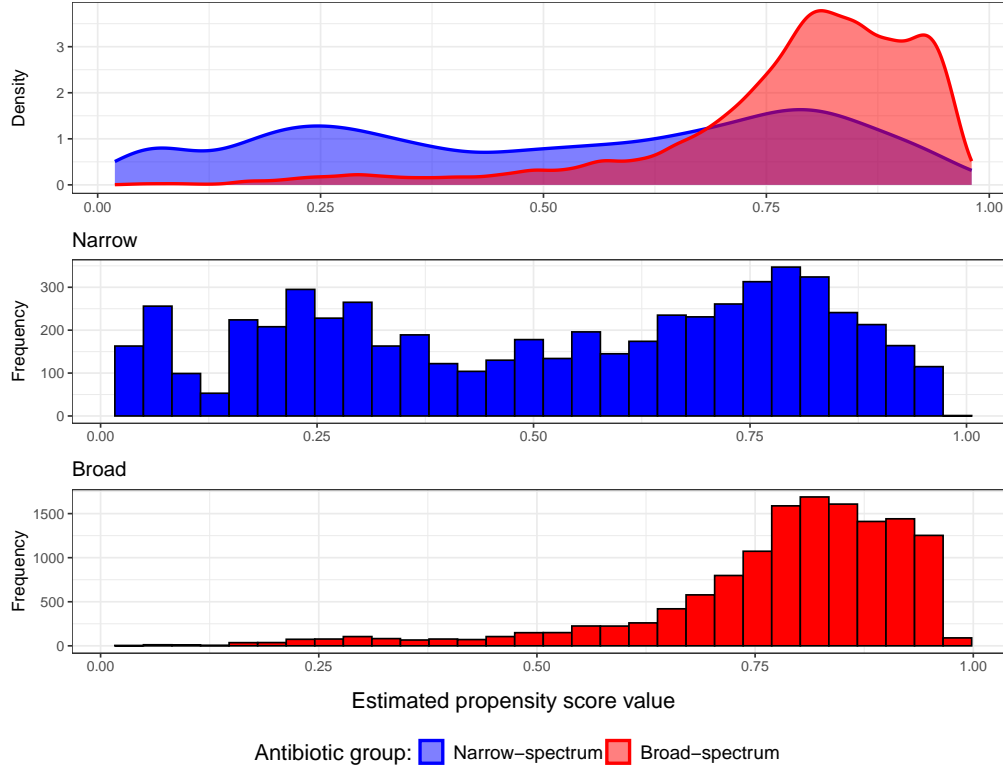
[†] Male is an indicator variable denoting whether the patient is a male. Arrival to culture and Arrival to treatment are indicators for whether arrival preceded culture collection or antibiotic treatment initiation, respectively, by more than two days. Previous ceftazidime culture is an indicator variable denoting whether a ceftazidime culture was taken before baseline.

Table A3: Logistic regression estimates from the propensity score model. OR: odds ratio; CI95%: 95% confidence intervals. Cefta: ceftazidime.

Covariate	OR	CI95%
Demographics		
Age	0.92	[0.90, 0.93]
Age ²	1.002	[1.0017, 1.0023]
Age ³	0.99999	[0.99998, 0.99999]
Male [†]	1.35	[1.26, 1.46]
Baseline sample location		
Other	1.00	
Not taken	1.39	[1.18, 1.64]
Multiple sources	2.26	[1.86, 2.75]
Urine	4.88	[4.09, 5.81]
Wound	0.24	[0.19, 0.29]
Blood	2.91	[2.32, 3.65]
Sputum	0.83	[0.64, 1.09]
Arrived from		
Other	1.00	
Home	0.75	[0.65, 0.85]
Institution	0.49	[0.42, 0.58]
Hospitalization unit		
Other	1.00	
Internal	7.84	[6.98, 8.80]
Surgical	5.99	[5.33, 6.75]
Medical history		
Dementia	0.85	[0.73, 0.98]
CRF	1.15	[1.01, 1.31]
Immunosuppression	1.07	[0.94, 1.22]
Diabetes	0.80	[0.73, 0.88]
Catheter	1.33	[1.19, 1.48]
Previous antibiotic use	0.91	[0.82, 1.01]
Previous cefta culture (365 days) [†]	0.78	[0.69, 0.88]
Medical information		
Arrival to culture (> 2 days) [†]	1.14	[1.04, 1.25]
Arrival to treatment (> 2 days) [†]	1.44	[1.31, 1.59]

[†] Male is an indicator variable denoting whether the patient is a male. Arrival to culture and Arrival to treatment are indicators for whether arrival preceded culture collection or antibiotic treatment initiation, respectively, by more than two days. Previous ceftazidime culture is an indicator variable denoting whether a ceftazidime culture was taken before baseline.

Figure A1: Estimated propensity score distribution by antibiotic-treatment group.



B Time-varying subpopulations

Beyond the stratification based on the one year post-treatment period, we can define different subpopulations as a function of other post-treatment periods r , with $r = 1$ being the special case analyzed in the main text. Let $S_i(a, r) = \mathbb{1}\{T_{i2}(a) > r\}$, and $I_i(a, r) = \mathbb{1}\{T_{i1}(a) \leq r\}$ be the survival and the resistant infection indicators, respectively, within the r -length time period under treatment level a .

For $a = 0, 1$, let $ios(r, a) = \{i : I_i(r, a) = 1 \cup S_i(r, a) = 1\}$. The subpopulation of patients that would have either acquired an infection or survived within the r -length period under both antibiotic treatments, which we term the *r-infected-or-survivors*, is then defined by $ios_r = \{i : i \in ios(r, 0) \cap ios(r, 1)\}$, with stratum proportion π_{ios_r} .

The proposed estimands can be then redefined to consider these time-varying subpopulations. For instance, the TV-FICE(t, r), the effect among the ios_r stratum, is defined (on the difference scale) by

$$\text{TV-FICE}(t, r) = \Pr[T_1(1) \leq t \mid ios_r] - \Pr[T_1(0) \leq t \mid ios_r], \quad (\text{A.1})$$

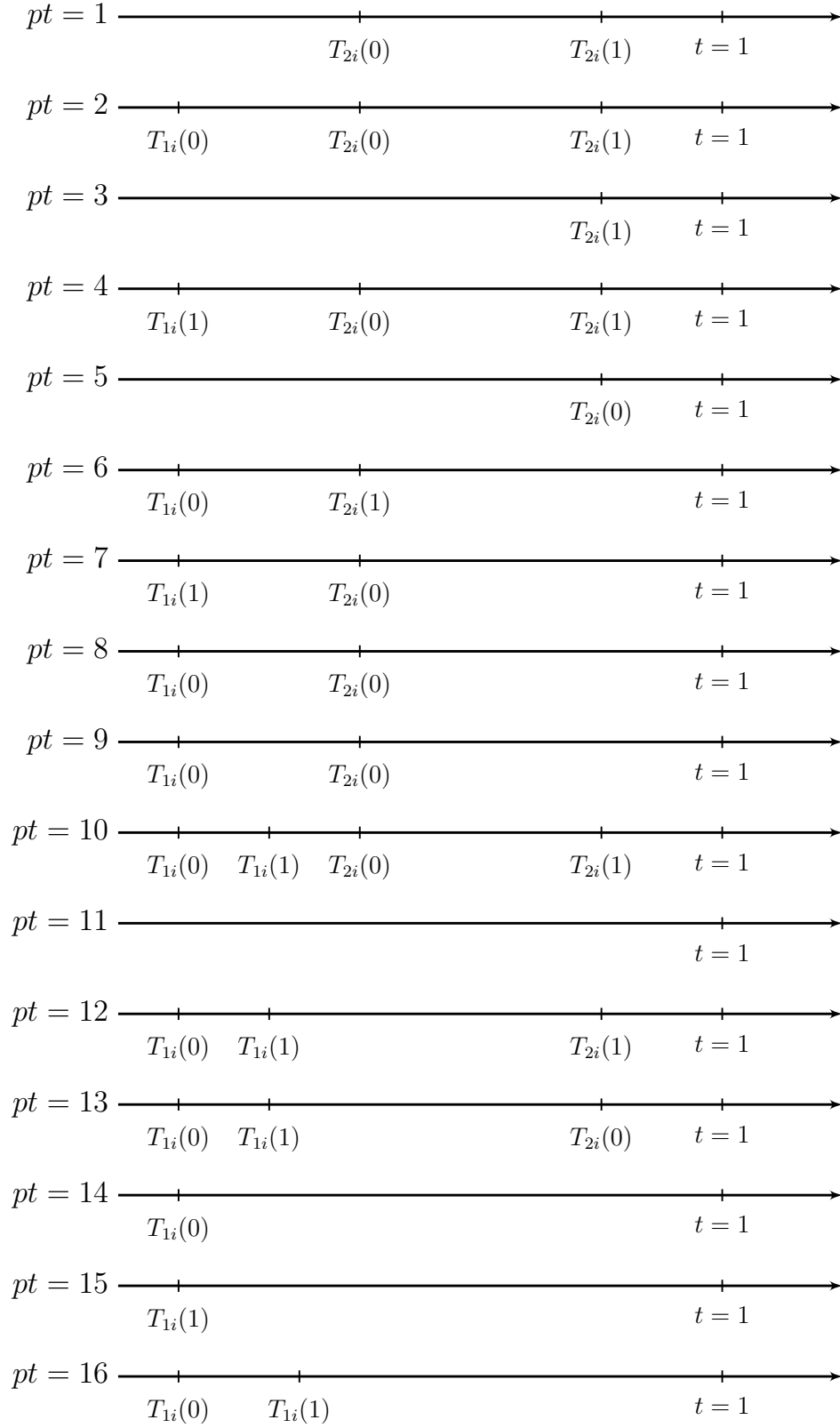
for $t \leq r$. The FICE(t), which we focus on in this paper, can be viewed as a special case of the TV-FICE(t, r), taking $r = 1$.

The proofs for the bounds can be generalized for each time-period r for which the ORP-type assumptions hold (see a short discussion in Section E.3). The extension for the identification under the frailty assumptions does not require any adjustment.

C Patient types illustration

Figure A2 provides an example of the possible event times of each patient type described in Table 2 of the main text. For simplicity of presentation only, in the examples below, if event j occurs under the Access antibiotic ($a = 0$), then $T_j(0) < T_j(1)$. Further, death times occur only after the last infection time (under both antibiotics). Of course, the ordering of the event times might be different as long as the quadruple of potential outcomes defining each patient type is preserved. For instance, $T_1(1)$ and/or $T_2(1)$ might be lower than $T_1(0)$.

Figure A2: Patient types illustration.



D Numerical examples

In this section, we present the results of a second simulation scenario we considered, and provide the parameter values and other relevant information about our numerical studies comparing the different estimands in synthetic DGMs. For both scenarios, the DGM was composed of hazard models, described by the Equations given by (2), with one continuous covariate and with Weibull baseline hazards. The bivariate frailty variable $\gamma = (\gamma_0, \gamma_1)$ was Gamma distributed, with $\theta := \theta_0 = \theta_1$. Scenarios were determined by the scale and shape parameters that govern the Weibull distribution of the baseline hazard functions, and the regression coefficients. The parameter values of each scenario are given in Table A4. For each scenario, we calculated the different causal estimands for several θ and ρ values.

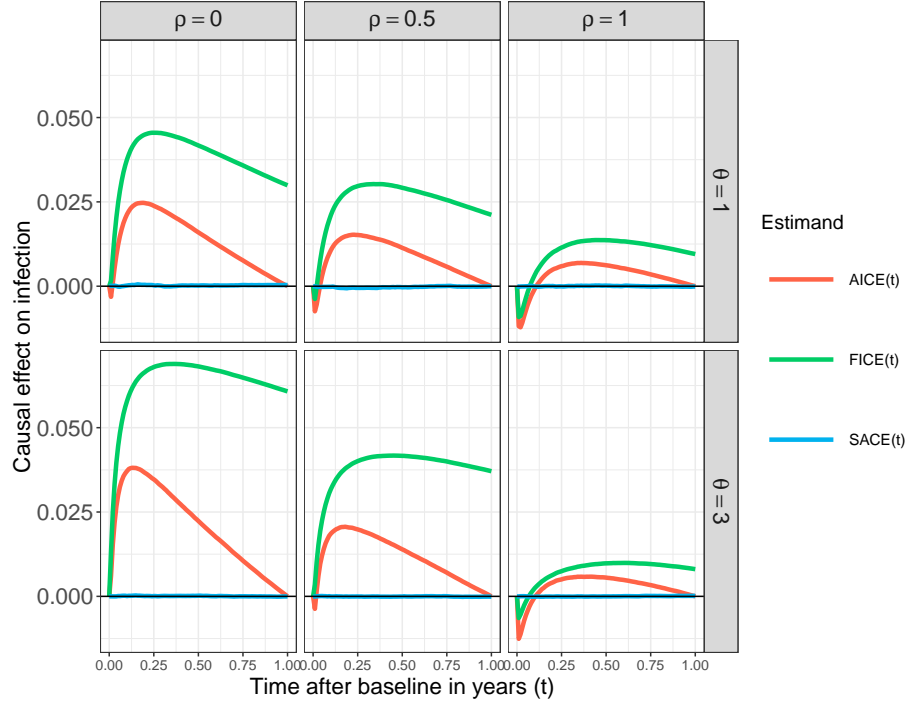
Figure A3 depicts the estimands under the new scenario (Scenario B). Compared with Scenario A, where the always-infected proportion was negligible (approximately 1%), in Scenario B this proportion was remarkably higher. For $\theta = 1$, the always-infected proportion ranged from 61% to 63%. For $\theta = 3$, although lower than under $\theta = 1$, it remained relatively high, varying between 35% and 44%. Importantly, the proportion of the ios stratum differed substantially from the proportion of always-survivors. The former was approximately 78% (under $\theta = 1$) and 82% (under $\theta = 3$), whereas the latter was lower than in Scenario A, ranging between 23% and 29% (under $\theta = 1$) and between 39% and 49% (under $\theta = 3$). Consequently, the FICE and the SACE diverged, in contrast to Scenario A where the ios and the always-survivors strata proportions were similar, and these strata substantially overlapped.

Interestingly, in Scenario B, the SACE remained zero throughout the entire one-year period, while both the FICE and the AICE were positive; their values increased during the first two months, and then declined. The magnitudes of these estimands diminished as ρ increased, with a more pronounced decrease under the higher θ value. This scenario illustrates that the value and trajectory over time of one estimand can diverge from those of the others, even when all underlying subpopulations are relatively large, and that the FICE is not necessarily monotone in time.

Table A4: Parameters for the data-generating mechanisms under Scenario A (presented in the main text) and Scenario B (presented in the Appendix), each with $\theta = 1, 3$ and $\rho = 0, 0.5, 1$. In every scenario, parameters for the Access group ($A = 0$) are shown in the first three rows, and parameters for the Watch group ($A = 1$) are shown in the last three rows.

Scenario	Baseline hazard shapes	Baseline hazard scales	Covariate coefficients
A	$\tilde{\alpha}_{01}^0 = 2.50$	$\tilde{\mu}_{01}^0 = 2.50$	$\beta_{01}^0 = (0.00, -0.69)$
	$\tilde{\alpha}_{02}^0 = 2.10$	$\tilde{\mu}_{02}^0 = 2.25$	$\beta_{02}^0 = (0.00, 0.69)$
	$\tilde{\alpha}_{12}^0 = 2.10$	$\tilde{\mu}_{12}^0 = 2.75$	$\beta_{12}^0 = (-0.69, 0.69)$
	$\tilde{\alpha}_{01}^1 = 2.50$	$\tilde{\mu}_{01}^1 = 2.00$	$\beta_{01}^1 = (-1.39, 1.10)$
	$\tilde{\alpha}_{02}^1 = 2.10$	$\tilde{\mu}_{02}^1 = 2.75$	$\beta_{02}^1 = (-0.29, 0.41)$
	$\tilde{\alpha}_{12}^1 = 2.10$	$\tilde{\mu}_{12}^1 = 2.25$	$\beta_{12}^1 = (0.00, 0.00)$
B	$\tilde{\alpha}_{01}^0 = 1.00$	$\tilde{\mu}_{01}^0 = 0.10$	$\beta_{01}^0 = (0.00, -0.69)$
	$\tilde{\alpha}_{02}^0 = 0.50$	$\tilde{\mu}_{02}^0 = 1.00$	$\beta_{02}^0 = (0.00, -0.69)$
	$\tilde{\alpha}_{12}^0 = 0.50$	$\tilde{\mu}_{12}^0 = 1.00$	$\beta_{12}^0 = (0.00, -0.69)$
	$\tilde{\alpha}_{01}^1 = 1.00$	$\tilde{\mu}_{01}^1 = 0.10$	$\beta_{01}^1 = (0.00, 0.69)$
	$\tilde{\alpha}_{02}^1 = 3.00$	$\tilde{\mu}_{02}^1 = 1.00$	$\beta_{02}^1 = (0.00, 0.69)$
	$\tilde{\alpha}_{12}^1 = 3.00$	$\tilde{\mu}_{12}^1 = 1.00$	$\beta_{12}^1 = (0.00, 0.69)$

Figure A3: Comparison of different estimands for a synthetic data-generating mechanism over one year following antibiotic treatment, Scenario B.



E FICE identification

E.1 Lemma for FICE identification

The following Lemma will be useful for the construction of the large-sample bounds and for identification under the frailty assumption. We provide the results for general r as defined in Section B. For constructing the bounds given in the main text, we will employ in Section E.3 this lemma with $r = 1$. For the frailty-based identification, we will employ the general version of the lemma in Section E.4. First, let

$$\pi_{ios_r} = \Pr \left(\left\{ \{T_1(0) \leq r\} \cup \{T_2(0) > r\} \right\} \cap \left\{ \{T_1(1) \leq r\} \cup \{T_2(1) > r\} \right\} \right) \quad (\text{A.2})$$

be the proportion of ios_r defined in Section B. We are now ready to present and prove the lemma.

Lemma A1. *For $a = 0, 1$, and for every $t \leq r$,*

$$\Pr \left(T_1(a) \leq t \mid ios_r \right) = \frac{\Pr \left(\left\{ T_1(a) \leq t \right\} \cap \left\{ \{T_1(1-a) \leq r\} \cup \{T_2(1-a) > r\} \right\} \right)}{\pi_{ios_r}}$$

Proof. For $a = 0, 1$ and for $t \leq r$,

$$\begin{aligned}
& \Pr(T_1(a) \leq t \mid ios_r) \\
&= \frac{\Pr\left(\{T_1(a) \leq t\} \cap \left\{\{T_1(a) \leq r\} \cup \{T_2(a) > r\}\right\} \cap \left\{\{T_1(1-a) \leq r\} \cup \{T_2(1-a) > r\}\right\}\right)}{\pi_{ios_r}} \\
&= \frac{\Pr\left(\{T_1(a) \leq t\} \cap \left\{\{T_1(1-a) \leq r\} \cup \{T_2(1-a) > r\}\right\}\right)}{\pi_{ios_r}}
\end{aligned} \tag{A.3}$$

where the second line is by the definition given in Equation A.2, and in the third line we used in the numerator that $\{T_1(a) \leq t\} \cup \left\{\{T_1(a) \leq r\} \cap \{T_2(a) > r\}\right\} = \{T_1(a) \leq t\}$ because $r \geq t$ (so $\{T_1(a) \leq t\}$ implies $\{T_1(a) \leq r\}$). \square

E.2 Results on ORP Assumptions

The following lemma compares the different estimands and asserts that weak-ORP is indeed the weakest of the three ORP-type assumptions.

Lemma A2. *Weak-ORP is a weaker assumption than ORP and weaker than ios-ORP.*

Proof. First, we show that ORP implies weak-ORP. From ORP, $I(0) = 1$ implies $I(1) = 1$. By the definition of $ios(1)$, if $I_i(1) = 1$, then $i \in ios(1)$. Putting it together, under ORP we have that for all i , $I_i(0) = 1$ implies $i \in ios(1)$. To show that weak-ORP does not imply ORP, we provide a counterexample. Patient type $pt = 8$ is not excluded by weak-ORP, but is excluded by ORP. Therefore, if $pt = 8$ exists, weak-ORP holds, whereas ORP does not, i.e., weak-ORP does not imply ORP.

We now show that ios-ORP implies weak-ORP. From the definition of $ios(0)$, if $I_i(0) = 1$ then $i \in ios(0)$. By ios-ORP, this means that $i \in ios(1)$. We obtain that under ios-ORP, $I_i(0) = 1$ implies $i \in ios(1)$ for all i . To show that weak-ORP does not imply ios-ORP, we provide another counterexample. Patient type $pt = 3$ is not excluded by weak-ORP, but is excluded by ios-ORP. Therefore, if $pt = 3$ exists, weak-ORP holds, whereas ios-ORP does not, i.e., weak-ORP does not imply ios-ORP. \square

E.3 Large-sample bounds for the FICE

In this section, we provide the proofs for partial identification of $FICE(t)$ with and without ORP-type assumptions.

We present the proofs for the estimands discussed in the main text, with time-fixed population. The results and proofs are immediately generalized to time-varying subpopulations, by replacing 1 with r , for every r such that $t \leq r \leq 1$. Note, however, that the ORP-type

assumptions change with r , and thus have to hold for the specific r in question for the results to be valid. As mentioned in Appendix B, the FICE(t), which we focus on in this paper, can be viewed as a special case of the TV-FICE(t, r) (defined in Equation A.1), taking $r = 1$.

The following Lemma provides bounds for the numerator of A.3, and will be used in the proofs of all the bounds we derive.

Lemma A3. *Under CE and consistency, for $a = 0, 1$,*

$$\mathcal{L}(a, t) \leq \Pr \left(\left\{ T_1(a) \leq t \right\} \cap \left\{ \{T_1(1-a) \leq 1\} \cup \{T_2(1-a) > 1\} \right\} \right) \leq \mathcal{U}(a, t)$$

where

$$\begin{aligned} \mathcal{L}(a, t) &= \max \left\{ 0, E_{\mathbf{X}} \left[\Psi_{A=1-a, \mathbf{X}} \right] - E_{\mathbf{X}} \left[S_{1|A=a, \mathbf{X}}(t) \right] \right\} \\ \mathcal{U}(a, t) &= \min \left\{ E_{\mathbf{X}} \left[F_{1|A=a, \mathbf{X}}(t) \right], E_{\mathbf{X}} \left[\Psi_{A=1-a, \mathbf{X}} \right] \right\}. \end{aligned}$$

Proof. The upper bound is obtained by

$$\begin{aligned} &\Pr \left(\left\{ T_1(a) \leq t \right\} \cap \left\{ \{T_1(1-a) \leq 1\} \cup \{T_2(1-a) > 1\} \right\} \right) \\ &\leq \min \left\{ \Pr \left(\left\{ T_1(a) \leq t \right\} \right), \Pr \left(\left\{ \{T_1(1-a) \leq 1\} \cup \{T_2(1-a) > 1\} \right\} \right) \right\} \\ &= \min \left\{ E_{\mathbf{X}} \left[F_{1|A=a, \mathbf{X}}(t) \right], E_{\mathbf{X}} \left[\Psi_{A=1-a, \mathbf{X}} \right] \right\}, \end{aligned}$$

where the second move is by the law of total expectation, CE, consistency and the definition of Ψ .

The lower bound is obtained by

$$\begin{aligned} &\Pr \left(\left\{ T_1(a) \leq t \right\} \cap \left\{ \{T_1(1-a) \leq 1\} \cup \{T_2(1-a) > 1\} \right\} \right) \\ &\geq \max \left\{ 0, \Pr \left(\left\{ T_1(a) \leq t \right\} \right) + \Pr \left(\left\{ \{T_1(1-a) \leq 1\} \cup \{T_2(1-a) > 1\} \right\} \right) - 1 \right\} \\ &= \max \left\{ 0, E_{\mathbf{X}} \left[\Psi_{A=1-a, \mathbf{X}} \right] - E_{\mathbf{X}} \left[S_{1|A=a, \mathbf{X}}(t) \right] \right\}, \end{aligned}$$

□

where the second move is by the law of total expectation, CE, and consistency and the definition of $S_{j|Q}(t)$.

E.3.1 Results under ios-ORP (Proposition 1)

Before proving Proposition 1, we present and prove the following lemma that will be useful for the proof. The lemma is of interest in its own right, as it shows that under ios-ORP, the proportion of *ios* in the population is identifiable.

Lemma A4. *Under CE, consistency and ios-ORP, the ios stratum proportion is identifiable by*

$$\pi_{ios} = E_{\mathbf{X}}[\Psi_{A=0, \mathbf{X}}]. \quad (\text{A.4})$$

Proof. We can write

$$\begin{aligned} \pi_{ios} &= \Pr\left(\left\{T_1(0) \leq 1\right\} \cup \left\{T_2(0) > 1\right\}\right) \\ &= E_{\mathbf{X}}\left[\Pr\left(\left\{T_1(0) \leq 1\right\} \cup \left\{T_2(0) > 1\right\} \mid \mathbf{X}\right)\right] \\ &= E_{\mathbf{X}}\left[\Pr\left(\left\{T_1(0) \leq 1\right\} \cup \left\{T_2(0) > 1\right\} \mid A = 0, \mathbf{X}\right)\right] \\ &= E_{\mathbf{X}}[\Psi_{A=0, \mathbf{X}}], \end{aligned}$$

where the first move is by ios-ORP, the second is by the law of total expectation, the third by CE and the final line is by consistency and the definition of Ψ . \square

We are now ready for the proof of Proposition 1.

E.3.1.1 Proof of Proposition 1

Proof. Starting from $\Pr(T_1(0) \leq t | ios)$, the denominator in Lemma A1, is identified by Lemma A4. Turning to the numerator, for every $t \leq 1$, $T_{i1}(0) \leq t$ implies that $i \in ios(0)$. Therefore, by ios-ORP, either $T_{i1}(1) \leq 1$ or $T_{i2}(1) > 1$. Hence,

$$\Pr\left(\left\{T_1(0) \leq t\right\} \cap \left\{\left\{T_1(1) \leq 1\right\} \cup \left\{T_2(1) > 1\right\}\right\}\right) = \Pr\left(\left\{T_1(0) \leq t\right\}\right) = E_{\mathbf{X}}\left[F_{1|A=0, \mathbf{X}}(t)\right],$$

where the second move is by the law of total expectation, CE, and consistency. Therefore, $\Pr(T_1(0) \leq t | ios)$ is identified by

$$\Pr(T_1(0) \leq t | ios) = \frac{E_{\mathbf{X}}\left[F_{1|A=0, \mathbf{X}}(t)\right]}{E_{\mathbf{X}}[\Psi_{A=0, \mathbf{X}}]}. \quad (\text{A.5})$$

Regarding $\Pr(T_1(1) \leq t | ios)$, we again employ Lemma A1; the denominator is identified by Lemma A4. To derive upper and lower bounds for the numerator, we apply Lemma A3 and obtain that

$$\max\left\{0, 1 - \frac{E_{\mathbf{X}}[S_{1|A=1, \mathbf{X}}(t)]}{E_{\mathbf{X}}[\Psi_{A=0, \mathbf{X}}]}\right\} \leq \Pr(T_1(1) \leq t | ios) \leq \min\left\{1, \frac{E_{\mathbf{X}}[F_{1|A=1, \mathbf{X}}(t)]}{E_{\mathbf{X}}[\Psi_{A=0, \mathbf{X}}]}\right\}. \quad (\text{A.6})$$

The proof is done by subtracting (A.5) from (A.6). \square

E.3.2 Results under weak-ORP (Proposition 2)

E.3.2.1 Bounds for the infected-or-survivors stratum proportion

Before providing FICE bounds, we first derive bounds for the ios stratum proportion under weak-ORP.

Lemma A5. *Under CE, consistency and weak-ORP, the ios stratum proportion is bounded by*

$$\tilde{\mathcal{L}}_\pi \leq \pi_{ios} \leq \tilde{\mathcal{U}}_\pi,$$

where

$$\begin{aligned}\tilde{\mathcal{L}}_\pi &= \max \left\{ E_{\mathbf{X}} \left[F_{1|A=0, \mathbf{X}}(1) \right], E_{\mathbf{X}} \left[\Psi_{A=0, \mathbf{X}} \right] + E_{\mathbf{X}} \left[\Psi_{A=1, \mathbf{X}} \right] - 1 \right\}, \\ \tilde{\mathcal{U}}_\pi &= \min \left\{ E_{\mathbf{X}} \left[\Psi_{A=0, \mathbf{X}} \right], E_{\mathbf{X}} \left[\Psi_{A=1, \mathbf{X}} \right] + E_{\mathbf{X}} \left[\Pr \left(\left\{ T_1 \leq 1 \right\} \cap \left\{ T_2 \leq 1 \right\} | A = 0, \mathbf{X} \right) \right] \right\}.\end{aligned}$$

Proof. First, we note that under weak-ORP, π_{ios} is equal to the difference between the $ios(0)$ subpopulation proportion and the proportion of $pt = 3$ (which is excluded by ios-ORP, but not by weak-ORP, and belongs to $ios(0)$, but not to the ios stratum). Therefore, an upper bound under weak-ORP can be derived by

$$\begin{aligned}\pi_{ios} &= \Pr \left(\left\{ T_1(0) \leq 1 \right\} \cup \left\{ T_2(0) > 1 \right\} \right) \\ &\quad - \Pr \left(\left\{ \left\{ T_1(0) > 1 \right\} \cap \left\{ T_2(0) > 1 \right\} \right\} \cap \left\{ \left\{ T_1(1) > 1 \right\} \cap \left\{ T_2(1) \leq 1 \right\} \right\} \right) \\ &= \Pr \left(\left\{ T_1(0) \leq 1 \right\} \cup \left\{ T_2(0) > 1 \right\} \right) \\ &\quad - \Pr \left(\left\{ T_2(0) > 1 \right\} \cap \left\{ \left\{ T_1(1) > 1 \right\} \cap \left\{ T_2(1) \leq 1 \right\} \right\} \right) \\ &\leq \Pr \left(\left\{ T_1(0) \leq 1 \right\} \cup \left\{ T_2(0) > 1 \right\} \right) \\ &\quad - \max \left\{ 0, \Pr \left(\left\{ T_2(0) > 1 \right\} \right) + \Pr \left(\left\{ T_1(1) > 1 \right\} \cap \left\{ T_2(1) \leq 1 \right\} \right) - 1 \right\} \\ &= \Pr \left(\left\{ T_1(0) \leq 1 \right\} \cup \left\{ T_2(0) > 1 \right\} \right) \\ &\quad - \max \left\{ 0, \Pr \left(\left\{ T_2(0) > 1 \right\} \right) - \Pr \left(\left\{ T_1(1) \leq 1 \right\} \cup \left\{ T_2(1) > 1 \right\} \right) \right\} \\ &= \min \left\{ \Pr \left(\left\{ T_1(0) \leq 1 \right\} \cup \left\{ T_2(0) > 1 \right\} \right), \right. \\ &\quad \left. \Pr \left(\left\{ T_1(1) \leq 1 \right\} \cup \left\{ T_2(1) > 1 \right\} \right) + \Pr \left(\left\{ T_1(0) \leq 1 \right\} \cap \left\{ T_2(0) \leq 1 \right\} \right) \right\} \\ &= \min \left\{ E_{\mathbf{X}} \left[\Psi_{A=0, \mathbf{X}} \right], E_{\mathbf{X}} \left[\Psi_{A=1, \mathbf{X}} \right] + E_{\mathbf{X}} \left[\Pr \left(\left\{ T_1(0) \leq 1 \right\} \cap \left\{ T_2(0) \leq 1 \right\} | A = 0, \mathbf{X} \right) \right] \right\},\end{aligned}\tag{A.7}$$

where the second move is by weak-ORP (with contrapositive); The fourth is because $\{T_1(1) \leq 1\} \cup \{T_2(1) > 1\}$ is the complementary of $\{T_1(1) > 1\} \cap \{T_2(1) \leq 1\}$; The fifth is because by $\Pr(A \cup B) = \Pr(A) + \Pr(B) - \Pr(A \cap B)$ (for two events A and B), along with the law of total probability, it follows that

$$\begin{aligned} & \Pr(\{T_1(0) \leq 1\} \cup \{T_2(0) > 1\}) - \Pr(\{T_2(0) > 1\}) \\ &= \Pr(\{T_1(0) \leq 1\}) - \Pr(\{T_1(0) \leq 1\} \cap \{T_2(0) > 1\}) = \Pr(\{T_1(0) \leq 1\} \cap \{T_2(0) \leq 1\}). \end{aligned}$$

Now, a lower bound under weak-ORP can be constructed by

$$\begin{aligned} \pi_{ios} &= \Pr(\{T_1(0) \leq 1\} \cup \{T_2(0) > 1\}) \\ &\quad - \Pr(\{T_1(0) > 1\} \cap \{T_2(0) > 1\}) \cap \{T_1(1) > 1\} \cap \{T_2(1) \leq 1\}) \\ &\geq \Pr(\{T_1(0) \leq 1\} \cup \{T_2(0) > 1\}) \\ &\quad - \min \left\{ \Pr(\{T_1(0) > 1\} \cap \{T_2(0) > 1\}), \Pr(\{T_1(1) > 1\} \cap \{T_2(1) \leq 1\}) \right\} \quad (\text{A.8}) \\ &= \max \left\{ \Pr(\{T_1(0) \leq 1\}), \right. \\ &\quad \left. \Pr(\{T_1(0) \leq 1\} \cup \{T_2(0) > 1\}) - \Pr(\{T_1(1) > 1\} \cap \{T_2(1) \leq 1\}) \right\} \\ &= \max \left\{ E_{\mathbf{X}}[F_{1|A=0,\mathbf{X}}(1)], E_{\mathbf{X}}[\Psi_{A=0,\mathbf{X}}] + E_{\mathbf{X}}[\Psi_{A=1,\mathbf{X}}] - 1 \right\}, \end{aligned}$$

where the third move is because by $\Pr(A \cap B) = \Pr(A) + \Pr(B) - \Pr(A \cup B)$ (for two events A and B), along with the law of total probability, it follows that

$$\begin{aligned} & \Pr(\{T_1(0) \leq 1\} \cup \{T_2(0) > 1\}) \\ & - \Pr(\{T_1(0) > 1\} \cap \{T_2(0) > 1\}) = \\ & \Pr(\{T_1(0) \leq 1\}) + \Pr(\{T_2(0) > 1\}) - \Pr(\{T_1(0) \leq 1\} \cap \{T_2(0) > 1\}) \\ & - \Pr(\{T_1(0) > 1\} \cap \{T_2(0) > 1\}) \\ & = \Pr(\{T_1(0) \leq 1\}), \end{aligned}$$

and the last move is due to the law of total expectation, CE, consistency and the definition of Ψ (and its complementary event). \square

Of note is that the upper bound under weak-ORP is lower than (or equal to) the expression identifying the *ios* stratum proportion under ios-ORP.

We are now ready for the proof of Proposition 2.

E.3.2.2 Proof of Proposition 2

Proof. We first provide upper and lower bounds, denoted by $\tilde{u}(t)$ and $\tilde{l}(t)$ respectively, for the difference between the numerators of Lemma A1, i.e. for

$$\Pr\left(\left\{T_1(1) \leq t\right\} \cap \left\{\left\{T_1(0) \leq 1\right\} \cup \left\{T_2(0) > 1\right\}\right\}\right) - \Pr\left(\left\{T_1(0) \leq t\right\} \cap \left\{\left\{T_1(1) \leq 1\right\} \cup \left\{T_2(1) > 1\right\}\right\}\right). \quad (\text{A.9})$$

Statrting with the first term ($a = 1$), we employ Lemma A3 to derive lower and upper bounds, i.e., $\mathcal{L}(1, t) \leq \Pr\left(\left\{T_1(1) \leq t\right\} \cap \left\{\left\{T_1(0) \leq 1\right\} \cup \left\{T_2(0) > 1\right\}\right\}\right) \leq \mathcal{U}(1, t)$.

For the second term ($a = 0$), we note that for every $t \leq 1$, $T_{i1}(0) \leq t$ implies that $T_{i1}(0) \leq 1$. Therefore, by weak-ORP, either $T_{i1}(1) \leq 1$ or $T_{i2}(1) > 1$. Hence,

$$\Pr\left(\left\{T_1(0) \leq t\right\} \cap \left\{\left\{T_1(1) \leq 1\right\} \cup \left\{T_2(1) > 1\right\}\right\}\right) = \Pr\left(\left\{T_1(0) \leq t\right\}\right) = E_{\mathbf{X}}\left[F_{1|A=0, \mathbf{X}}(t)\right], \quad (\text{A.10})$$

where the second move is by the law of total expectation, CE, and consistency. Of note is that the proofs for each of the numerators of Lemma A1 under weak-ORP are identical to the proofs of Proposition 1 (i.e., under ios-ORP).

The upper and lower bounds for the difference in A.9, $\tilde{u}(t)$ and $\tilde{l}(t)$, are obtained by subtracting (A.10) from $\mathcal{U}(1, t)$ and from $\mathcal{L}(1, t)$, respectively,

$$\begin{aligned} \tilde{u}(t) &= \min\left\{E_{\mathbf{X}}\left[F_{1|A=1, \mathbf{X}}(t)\right], E_{\mathbf{X}}\left[\Psi_{A=0, \mathbf{X}}(1)\right]\right\} - E_{\mathbf{X}}\left[F_{1|A=0, \mathbf{X}}(t)\right], \\ \tilde{l}(t) &= \max\left\{0, E_{\mathbf{X}}\left[\Psi_{A=0, \mathbf{X}}(1)\right] - E_{\mathbf{X}}\left[S_{1|A=1, \mathbf{X}}(t)\right]\right\} - E_{\mathbf{X}}\left[F_{1|A=0, \mathbf{X}}(t)\right], \end{aligned} \quad (\text{A.11})$$

with $1\{\cdot\}$ being the indicator function.

To obtain FICE bound, we tie (A.11) together with Lemma A1 and the bounds for π_{ios} under weak-ORP, given in Lemma A5. For the upper FICE bound, if $\tilde{u}(t)$ is positive, we divide it by $\tilde{\mathcal{L}}_{\pi}$. Otherwise, we divide it by $\tilde{\mathcal{U}}_{\pi}$. For the lower FICE bound, if $\tilde{l}(t)$ is positive, we divide it by $\tilde{\mathcal{U}}_{\pi}$. Otherwise, we divide it by $\tilde{\mathcal{L}}_{\pi}$. \square

E.3.3 Results without ORP-type assumptions (Proposition A1)

Before providing FICE bounds, we first derive bounds for the ios stratum proportion without ORP-type assumptions.

Lemma A6. *Under CE and consistency, the ios stratum proportion is bounded by*

$$\dot{\mathcal{L}}_{\pi} \leq \pi_{ios} \leq \dot{\mathcal{U}}_{\pi},$$

where

$$\begin{aligned} \dot{\mathcal{L}}_{\pi} &= \max\left\{0, E_{\mathbf{X}}\left[\Psi_{A=0, \mathbf{X}}\right] + E_{\mathbf{X}}\left[\Psi_{A=1, \mathbf{X}}\right] - 1\right\}, \\ \dot{\mathcal{U}}_{\pi} &= \min_a \left\{E_{\mathbf{X}}\left[\Psi_{A=a, \mathbf{X}}\right]\right\}. \end{aligned}$$

Proof. First,

$$\begin{aligned}\pi_{ios} &\leq \min_a \left\{ \Pr \left(\left\{ \{T_1(a) \leq 1\} \cup \{T_2(a) > 1\} \right\} \right) \right\} \\ &= \min_a \left\{ E_{\mathbf{X}} [\Psi_{A=a, \mathbf{X}}] \right\},\end{aligned}$$

where the second move is by the law of total expectation, CE, and consistency.

Second,

$$\begin{aligned}\pi_{ios} &\geq \max \left\{ 0, \Pr \left(\left\{ \{T_1(0) \leq 1\} \cup \{T_2(0) > 1\} \right\} \right) + \Pr \left(\left\{ \{T_1(1) \leq 1\} \cup \{T_2(1) > 1\} \right\} \right) - 1 \right\} \\ &= \max \left\{ 0, E_{\mathbf{X}} [\Psi_{A=0, \mathbf{X}}] + E_{\mathbf{X}} [\Psi_{A=1, \mathbf{X}}] - 1 \right\},\end{aligned}$$

where the last move is due to the law of total expectation, CE, consistency and definition of Ψ . \square

Similarly to the upper bound under weak-ORP (Lemma A5), the upper bound without ORP assumptions is lower than (or equal to) the expression identifying the *ios* stratum proportion under ios-ORP.

Furthermore, the upper bound without ORP assumptions is lower than (or equal to) its counterpart under weak-ORP. When $E_{\mathbf{X}} [\Psi_{A=0, \mathbf{X}}] \leq E_{\mathbf{X}} [\Psi_{A=1, \mathbf{X}}]$, the upper bounds coincide and equal to the proportion under ios-ORP, that is, $E_{\mathbf{X}} [\Psi_{A=0, \mathbf{X}}]$. This is the case in our motivating dataset. The lower bounds without ORP assumptions and under weak-ORP were also identical in the motivating dataset.

We now turn to provide FICE bounds without ORP-type assumptions.

Proposition A1. *Under consistency and CE, the FICE(t) is bounded by*

$$\dot{\mathcal{L}}(t) \leq FICE(t) \leq \dot{\mathcal{U}}(t),$$

$$\text{where } \dot{\mathcal{U}}(t) = \frac{\dot{u}(t)}{1\{\dot{u}(t) \geq 0\} \cdot \dot{\mathcal{L}}_{\pi} + 1\{\dot{u}(t) < 0\} \cdot \dot{\mathcal{U}}_{\pi}}, \dot{\mathcal{L}}(t) = \frac{\dot{l}(t)}{1\{\dot{l}(t) \geq 0\} \cdot \dot{\mathcal{U}}_{\pi} + 1\{\dot{l}(t) < 0\} \cdot \dot{\mathcal{L}}_{\pi}},$$

and

$$\begin{aligned}\dot{u}(t) &= \min \left\{ E_{\mathbf{X}} [F_{1|A=1, \mathbf{X}}(t)], E_{\mathbf{X}} [\Psi_{A=0, \mathbf{X}}] \right\} - \max \left\{ 0, E_{\mathbf{X}} [\Psi_{A=1, \mathbf{X}}] - E_{\mathbf{X}} [S_{1|A=0, \mathbf{X}}(t)] \right\}, \\ \dot{l}(t) &= \max \left\{ 0, E_{\mathbf{X}} [\Psi_{A=0, \mathbf{X}}] - E_{\mathbf{X}} [S_{1|A=1, \mathbf{X}}(t)] \right\} - \min \left\{ E_{\mathbf{X}} [F_{1|A=0, \mathbf{X}}(t)], E_{\mathbf{X}} [\Psi_{A=1, \mathbf{X}}] \right\}.\end{aligned}$$

Note that both $\dot{u}(t)$ and $\dot{l}(t)$ are higher than (or equal to) their counterparts under weak-ORP, $\tilde{u}(t)$ and $\tilde{l}(t)$.

Proof. We first derive upper and lower bounds for the difference between the numerators of Lemma A1, i.e. for

$$\Pr\left(\left\{T_1(1) \leq t\right\} \cap \left\{\left\{T_1(0) \leq 1\right\} \cup \left\{T_2(0) > 1\right\}\right\}\right) - \Pr\left(\left\{T_1(0) \leq t\right\} \cap \left\{\left\{T_1(1) \leq 1\right\} \cup \left\{T_2(1) > 1\right\}\right\}\right). \quad (\text{A.12})$$

Employing Lemma A3 with both $a = 0$ and $a = 1$, the upper bound for (A.12) is obtained by subtracting the lower bound of the second term ($a = 0$) from the upper bound of the first term ($a = 1$),

$$\dot{u}(t) = \min\left\{E_{\mathbf{X}}\left[F_{1|A=1,\mathbf{X}}(t)\right], E_{\mathbf{X}}\left[\Psi_{A=0,\mathbf{X}}\right]\right\} - \max\left\{0, E_{\mathbf{X}}\left[\Psi_{A=1,\mathbf{X}}\right] - E_{\mathbf{X}}\left[S_{1|A=0,\mathbf{X}}(t)\right]\right\}. \quad (\text{A.13})$$

Similarly, the lower bound for (A.12) is obtained by subtracting the upper bound of the second term ($a = 0$) from the lower bound of the first term ($a = 1$),

$$\dot{l}(t) = \max\left\{0, E_{\mathbf{X}}\left[\Psi_{A=0,\mathbf{X}}\right] - E_{\mathbf{X}}\left[S_{1|A=1,\mathbf{X}}(t)\right]\right\} - \min\left\{E_{\mathbf{X}}\left[F_{1|A=0,\mathbf{X}}(t)\right], E_{\mathbf{X}}\left[\Psi_{A=1,\mathbf{X}}\right]\right\}. \quad (\text{A.14})$$

To obtain FICE bound, we tie (A.13) and (A.14) together with Lemma A1 and the bounds for π_{ios} of Lemma A6. For the upper FICE bound, if $\dot{u}(t)$ is positive, we divide it by $\dot{\mathcal{L}}_{\pi}$. Otherwise, we divide it by $\dot{\mathcal{U}}_{\pi}$. For the lower FICE bound, if $\dot{l}(t)$ is positive, we divide it by $\dot{\mathcal{U}}_{\pi}$. Otherwise, we divide it by $\dot{\mathcal{L}}_{\pi}$. \square

E.3.4 Bounds for the risk-ratio scale FICE(t) (Propositions A2 and A3)

Proposition A2. *Under consistency, CE and weak-ORP (or ios-ORP), the risk-ratio scale FICE(t) is bounded by*

$$\left[\frac{\max\left\{0, E_{\mathbf{X}}\left[\Psi_{A=0,\mathbf{X}}\right] - E_{\mathbf{X}}\left[S_{1|A=1,\mathbf{X}}(t)\right]\right\}}{E_{\mathbf{X}}\left[F_{1|A=0,\mathbf{X}}(t)\right]}, \frac{\min\left\{E_{\mathbf{X}}\left[\Psi_{A=0,\mathbf{X}}\right], E_{\mathbf{X}}\left[F_{1|A=1,\mathbf{X}}(t)\right]\right\}}{E_{\mathbf{X}}\left[F_{1|A=0,\mathbf{X}}(t)\right]} \right].$$

Proof. Applying Lemma A1 for both $\Pr\left(T_1(1) \leq t \mid ios\right)$ and $\Pr\left(T_1(0) \leq t \mid ios\right)$, it follows

that the ratio $\frac{\Pr\left(\left\{T_1(1) \leq t\right\} \mid ios\right)}{\Pr\left(\left\{T_1(0) \leq t\right\} \mid ios\right)}$ can be written as

$$\frac{\Pr\left(\left\{T_1(1) \leq t\right\} \mid ios\right)}{\Pr\left(\left\{T_1(0) \leq t\right\} \mid ios\right)} = \frac{\Pr\left(\left\{T_1(1) \leq t\right\} \cap \left\{\left\{T_1(0) \leq 1\right\} \cup \left\{T_2(0) > 1\right\}\right\}\right)}{\Pr\left(\left\{T_1(0) \leq t\right\} \cap \left\{\left\{T_1(1) \leq 1\right\} \cup \left\{T_2(1) > 1\right\}\right\}\right)}. \quad (\text{A.15})$$

To derive upper and lower bounds for the numerator of (A.15), we employ Lemma A3 (with $a = 1$) to obtain

$$\mathcal{L}(1, t) \leq \Pr \left(\left\{ T_1(1) \leq t \right\} \cap \left\{ \left\{ T_1(0) \leq 1 \right\} \cup \left\{ T_2(0) > 1 \right\} \right\} \right) \leq \mathcal{U}(1, t), \quad (\text{A.16})$$

where

$$\begin{aligned} \mathcal{L}(1, t) &= \max \left\{ 0, E_{\mathbf{X}} [\Psi_{A=0, \mathbf{X}}] - E_{\mathbf{X}} [S_{1|A=1, \mathbf{X}}(t)] \right\}, \\ \mathcal{U}(1, t) &= \min \left\{ E_{\mathbf{X}} [\Psi_{A=0, \mathbf{X}}], E_{\mathbf{X}} [F_{1|A=1, \mathbf{X}}(t)] \right\}. \end{aligned}$$

The denominator of (A.15), i.e. for $a = 0$, is identified by

$$\Pr \left(\left\{ T_1(0) \leq t \right\} \cap \left\{ \left\{ T_1(1) \leq 1 \right\} \cup \left\{ T_2(1) > 1 \right\} \right\} \right) = \Pr \left(\left\{ T_1(0) \leq t \right\} \right) = E_{\mathbf{X}} [F_{1|A=0, \mathbf{X}}(t)], \quad (\text{A.17})$$

where the first move is by weak-ORP (and because for every $t \leq 1$, $T_{i1}(0) \leq t$ implies that $T_{i1}(0) \leq 1$), and the second is by the law of total expectation, CE, and consistency. The proof is done by dividing (A.16) by (A.17).

We note that on the risk-ratio scale, identification of π_{ios} is not required, as it cancels out. Hence, the bounds under ios-ORP and weak-ORP coincide, because only the (full/partial) identification of π_{ios} distinguishes between them. \square

Proposition A3. *Under consistency and CE, the risk-ratio scale FICE(t) is bounded by*

$$\left[\frac{\max \left\{ 0, E_{\mathbf{X}} [\Psi_{A=0, \mathbf{X}}] - E_{\mathbf{X}} [S_{1|A=1, \mathbf{X}}(t)] \right\}}{\min \left\{ E_{\mathbf{X}} [\Psi_{A=1, \mathbf{X}}], E_{\mathbf{X}} [F_{1|A=0, \mathbf{X}}(t)] \right\}}, \frac{\min \left\{ E_{\mathbf{X}} [F_{1|A=1, \mathbf{X}}(t)], E_{\mathbf{X}} [\Psi_{A=0, \mathbf{X}}] \right\}}{\max \left\{ 0, E_{\mathbf{X}} [\Psi_{A=1, \mathbf{X}}] - E_{\mathbf{X}} [S_{1|A=0, \mathbf{X}}(t)] \right\}} \right]. \quad (\text{A.18})$$

Proof. Applying Lemma A1 for both $\Pr (T_1(1) \leq t \mid ios)$ and $\Pr (T_1(0) \leq t \mid ios)$, it follows that the ratio $\frac{\Pr (\{T_1(1) \leq t\} \mid ios)}{\Pr (\{T_1(0) \leq t\} \mid ios)}$ can be written as

$$\frac{\Pr (\{T_1(1) \leq t\} \mid ios)}{\Pr (\{T_1(0) \leq t\} \mid ios)} = \frac{\Pr (\{T_1(1) \leq t\} \cap \{ \{T_1(0) \leq 1\} \cup \{T_2(0) > 1\} \})}{\Pr (\{T_1(0) \leq t\} \cap \{ \{T_1(1) \leq 1\} \cup \{T_2(1) > 1\} \})}. \quad (\text{A.19})$$

Similarly to the proof of Proposition A2, to derive upper and lower bounds for the numerator of (A.19), we employ Lemma A3 with $a = 1$,

$$\mathcal{L}(1, t) \leq \Pr \left(\left\{ T_1(1) \leq t \right\} \cap \left\{ \left\{ T_1(0) \leq 1 \right\} \cup \left\{ T_2(0) > 1 \right\} \right\} \right) \leq \mathcal{U}(1, t), \quad (\text{A.20})$$

where

$$\begin{aligned} \mathcal{L}(1, t) &= \max \left\{ 0, E_{\mathbf{X}} [\Psi_{A=0, \mathbf{X}}] - E_{\mathbf{X}} [S_{1|A=1, \mathbf{X}}(t)] \right\} \\ \mathcal{U}(1, t) &= \min \left\{ E_{\mathbf{X}} [\Psi_{A=0, \mathbf{X}}], E_{\mathbf{X}} [F_{1|A=1, \mathbf{X}}(t)] \right\}. \end{aligned}$$

Now, for upper and lower bounds for the denominator of (A.19), we employ Lemma A3 with $a = 0$,

$$\mathcal{L}(0, t) \leq \Pr \left(\left\{ T_1(0) \leq t \right\} \cap \left\{ \left\{ T_1(1) \leq 1 \right\} \cup \left\{ T_2(1) > 1 \right\} \right\} \right) \leq \mathcal{U}(0, t), \quad (\text{A.21})$$

where

$$\begin{aligned} \mathcal{L}(0, t) &= \max \left\{ 0, E_{\mathbf{X}} \left[\Psi_{A=1, \mathbf{X}} \right] - E_{\mathbf{X}} \left[S_{1|A=0, \mathbf{X}}(t) \right] \right\} \\ \mathcal{U}(0, t) &= \min \left\{ E_{\mathbf{X}} \left[\Psi_{A=1, \mathbf{X}} \right], E_{\mathbf{X}} \left[F_{1|A=0, \mathbf{X}}(t) \right] \right\}. \end{aligned}$$

To finish the proof, we tie (A.19) together with (A.20) and (A.21). The upper FICE bound is obtained by $\frac{\mathcal{U}(1, t)}{\mathcal{L}(0, t)}$. The lower FICE bound is obtained by $\frac{\mathcal{L}(1, t)}{\mathcal{U}(0, t)}$. \square

E.4 Identification under the frailty assumptions

E.4.1 Results for the TV-FICE(t, r) under the frailty assumptions (Proposition 3)

We now present the proof for the identification formula of the TV-FICE(t, r) under the frailty assumptions. Here, we consider the time-varying population, determined by the r value. As noted in Section E.3, the FICE(t) can be viewed as a special case of the TV-FICE(t, r), taking $r = 1$. In contrast to the case under the ORP-type assumptions, frailty assumptions require no modification, i.e., the frailty assumptions are sufficient for identification of the TV-FICE(t, r) as a function of ρ in all the subpopulations.

Proof. By the law of total expectation and by the definition of π_{iosr} , Equation (A.3) of Lemma A1 can be written as

$$\frac{E_{\mathbf{X}, \gamma} \left[\Pr \left(\left\{ T_1(a) \leq t \right\} \cap \left\{ \left\{ T_1(1-a) \leq r \right\} \cup \left\{ T_2(1-a) > r \right\} \right\} \middle| \mathbf{X}, \gamma \right) \right]}{E_{\mathbf{X}, \gamma} \left[\Pr \left(\left\{ \left\{ T_1(0) \leq r \right\} \cup \left\{ T_2(0) > r \right\} \right\} \cap \left\{ \left\{ T_1(1) \leq r \right\} \cup \left\{ T_2(1) > r \right\} \right\} \middle| \mathbf{X}, \gamma \right) \right]}. \quad (\text{A.22})$$

Now, Equation (A.22) can be replaced with

$$\begin{aligned}
& \frac{E_{\mathbf{X}, \gamma} \left[\Pr \left(\{T_1 \leq t\} \middle| A = a, \mathbf{X}, \gamma_a \right) \Pr \left(\{ \{T_1 \leq r\} \cup \{T_2 > r\} \} \middle| A = 1 - a, \mathbf{X}, \gamma_{1-a} \right) \right]}{E_{\mathbf{X}, \gamma} \left[\Pr \left(\{ \{T_1 \leq r\} \cup \{T_2 > r\} \} \middle| A = 0, \mathbf{X}, \gamma_0 \right) \Pr \left(\{ \{T_1 \leq r\} \cup \{T_2 > r\} \} \middle| A = 1, \mathbf{X}, \gamma_1 \right) \right]} \\
&= \frac{\int_{\mathbf{x}} \int_{\gamma_0} \int_{\gamma_1} \Pr \left(\{T_1 \leq t\} \middle| A = a, \mathbf{X} = \mathbf{x}, \gamma_a \right) \Pr \left(\{ \{T_1 \leq r\} \cup \{T_2 > r\} \} \middle| A = 1 - a, \mathbf{X} = \mathbf{x}, \gamma_{1-a} \right) f(\gamma, \mathbf{x}) d\gamma_1 d\gamma_0 d\mathbf{x}}{\int_{\mathbf{x}} \left\{ \int_{\gamma_0} \int_{\gamma_1} \Pr \left(\{ \{T_1 \leq r\} \cup \{T_2 > r\} \} \middle| A = 0, \mathbf{X} = \mathbf{x}, \gamma_0 \right) \Pr \left(\{ \{T_1 \leq r\} \cup \{T_2 > r\} \} \middle| A = 1, \mathbf{X} = \mathbf{x}, \gamma_1 \right) \right.} \\
&\quad \cdot f(\gamma, \mathbf{x}) d\gamma_1 d\gamma_0 d\mathbf{x} \left. \right\}}{\int_{\mathbf{x}} f(\mathbf{x}) \int_{\gamma_0} \int_{\gamma_1} \Pr \left(\{T_1 \leq t\} \middle| A = a, \mathbf{X} = \mathbf{x}, \gamma_a \right) \Pr \left(\{ \{T_1 \leq r\} \cup \{T_2 > r\} \} \middle| A = 1 - a, \mathbf{X} = \mathbf{x}, \gamma_{1-a} \right) f_{\theta}(\gamma) d\gamma_1 d\gamma_0 d\mathbf{x}} \\
&= \frac{\int_{\mathbf{x}} \left\{ f(\mathbf{x}) \int_{\gamma_0} \int_{\gamma_1} \Pr \left(\{ \{T_1 \leq r\} \cup \{T_2 > r\} \} \middle| A = 0, \mathbf{X} = \mathbf{x}, \gamma_0 \right) \Pr \left(\{ \{T_1 \leq r\} \cup \{T_2 > r\} \} \middle| A = 1, \mathbf{X} = \mathbf{x}, \gamma_1 \right) \right.} \\
&\quad \cdot f_{\theta}(\gamma) d\gamma_1 d\gamma_0 d\mathbf{x} \left. \right\}}{E_{\mathbf{X}} \left[E_{\gamma} \left[\Pr \left(\{T_1 \leq t\} \middle| A = a, \mathbf{X}, \gamma_a \right) \Pr \left(\{ \{T_1 \leq r\} \cup \{T_2 > r\} \} \middle| A = 1 - a, \mathbf{X}, \gamma_{1-a} \right) \right] \right]} \\
&= \frac{E_{\mathbf{X}} \left[E_{\gamma} \left[\Pr \left(\{T_1 \leq t\} \middle| A = a, \mathbf{X}, \gamma_a \right) \Pr \left(\{ \{T_1 \leq r\} \cup \{T_2 > r\} \} \middle| A = 1 - a, \mathbf{X}, \gamma_{1-a} \right) \right] \right]}{E_{\mathbf{X}} \left[E_{\gamma} \left[\Pr \left(\{ \{T_1 \leq r\} \cup \{T_2 > r\} \} \middle| A = 0, \mathbf{X}, \gamma_0 \right) \Pr \left(\{ \{T_1 \leq r\} \cup \{T_2 > r\} \} \middle| A = 1, \mathbf{X}, \gamma_1 \right) \right] \right]}, \tag{A.23}
\end{aligned}$$

where the first term is due to parts (i) and (ii) of the frailty assumptions, together with consistency, the third is by part (iii) of the frailty assumptions, and where $f(\gamma, \mathbf{x})$ is the joint density function of γ and \mathbf{X} , $f(\mathbf{x})$ is the density function of \mathbf{X} and $f_{\theta}(\gamma)$ is the density function of γ . \square

E.4.2 Results for the risk-ratio scale TV-FICE(t, r) under the frailty assumptions (Proposition A4)

Proposition A4. *Under the frailty assumptions, the risk-ratio scale TV-FICE(t, r) is identified by*

$$\frac{E_{\mathbf{X}} \left[E_{\gamma} \left[\Pr \left(\{T_1 \leq t\} \middle| A = 1, \mathbf{X}, \gamma_1 \right) \Pr \left(\{ \{T_1 \leq r\} \cup \{T_2 > r\} \} \middle| A = 0, \mathbf{X}, \gamma_0 \right) \right] \right]}{E_{\mathbf{X}} \left[E_{\gamma} \left[\Pr \left(\{T_1 \leq t\} \middle| A = 0, \mathbf{X}, \gamma_0 \right) \Pr \left(\{ \{T_1 \leq r\} \cup \{T_2 > r\} \} \middle| A = 1, \mathbf{X}, \gamma_1 \right) \right] \right]}.$$

Proof. The risk-ratio scale estimand is obtained by taking the ratio between the term in (A.23) with $a = 1$ and the same term with $a = 0$. The denominator cancels out, so we divide the numerators of both terms to obtain the risk-ratio scale TV-FICE(t, r) bounds. \square

F Estimation

F.1 Derivation of the likelihood function

For completeness, we derive here the likelihood function for the illness-death models. In practice it is maximized by an EM algorithm. First, recall the notations adopted for the parameters in Section 5; $\tilde{\boldsymbol{\theta}} = (\theta_0, \theta_1)$, $\tilde{\boldsymbol{\beta}} = (\boldsymbol{\beta}^0, \boldsymbol{\beta}^1)$, $\tilde{\boldsymbol{\lambda}}_0(t) = (\boldsymbol{\lambda}^0(t), \boldsymbol{\lambda}^1(t))$, and $\tilde{\boldsymbol{\Lambda}}_0(t) = (\boldsymbol{\Lambda}^0(t), \boldsymbol{\Lambda}^1(t))$, where, for $a = 0, 1$, $\boldsymbol{\beta}^a = (\beta_{01}^a, \beta_{02}^a, \beta_{12}^a)$, $\boldsymbol{\lambda}^a(t) = (\lambda_{01}^0(t|a), \lambda_{02}^0(t|a), \lambda_{12}^0(t|a))$, and $\boldsymbol{\Lambda}^a(t) = (\Lambda_{01}^0(t|a), \Lambda_{02}^0(t|a), \Lambda_{12}^0(t|a))$.

Under the hazard models described in Equation (2), the likelihood function, integrated over the frailty distribution, equals $L(\tilde{\boldsymbol{\theta}}, \tilde{\boldsymbol{\Lambda}}_0, \tilde{\boldsymbol{\lambda}}_0, \tilde{\boldsymbol{\beta}}) = \prod_{i=1}^n L_i$, where

$$\begin{aligned}
L_i &= \int_0^\infty f(\tilde{T}_{i1}, \tilde{T}_{i2}, \delta_{i1}, \delta_{i2}, \gamma_{A_i} | \mathbf{X}_i) d\gamma_{A_i} \\
&= \int_0^\infty f(\tilde{T}_{i1}, \tilde{T}_{i2}, \delta_{i1}, \delta_{i2} | \mathbf{X}_i, \gamma_{A_i}) f(\gamma_{A_i} | \mathbf{X}_i) d\gamma_{A_i} = \int_0^\infty f(\tilde{T}_{i1}, \tilde{T}_{i2}, \delta_{i1}, \delta_{i2}, | \mathbf{X}_i, \gamma_{A_i}) f(\gamma_{A_i}) d\gamma_{A_i} \\
&= \int_0^\infty \left[\lambda_{01}(\tilde{T}_{i1} | A_i, \mathbf{X}_i, \gamma_{A_i}) \right]^{\delta_{i1}} \left[\lambda_{02}(\tilde{T}_{i1} | A_i, \mathbf{X}_i, \gamma_{A_i}) \right]^{(1-\delta_{i1})\delta_{i2}} \left[\lambda_{12}(\tilde{T}_{i2} | A_i, \mathbf{X}_i, \gamma_{A_i}) \right]^{\delta_{i1}\delta_{i2}} \\
&\quad \exp \left\{ - [H_{01}(\tilde{T}_{i1} | A_i, \mathbf{X}_i, \gamma_{A_i}) + H_{02}(\tilde{T}_{i1} | a_i, \mathbf{X}_i, \gamma_{A_i}) + \delta_1 (H_{12}(\tilde{T}_{i2} | a_i, \mathbf{X}_i, \gamma_{A_i}) - H_{12}(\tilde{T}_{i1} | A_i, \mathbf{X}_i, \gamma_{A_i}))] \right\} \\
&\quad f(\gamma_{A_i}) d\gamma_{A_i} \\
&= \int_0^\infty \left[\gamma_{A_i} \lambda_{01}^0(\tilde{T}_{i1} | A_i) \exp(\mathbf{X}_i^t \boldsymbol{\beta}_{01}^{A_i}) \right]^{\delta_{i1}} \left[\gamma_{A_i} \lambda_{02}^0(\tilde{T}_{i2} | A_i) \exp(\mathbf{X}_i^t \boldsymbol{\beta}_{02}^{A_i}) \right]^{(1-\delta_{i1})\delta_{i2}} \left[\gamma_{A_i} \lambda_{12}^0(\tilde{T}_{i2} | A_i) \exp(\mathbf{X}_i^t \boldsymbol{\beta}_{12}^{A_i}) \right]^{\delta_{i1}\delta_{i2}} \\
&\quad \exp \left\{ - \gamma_{A_i} \left[\left(H_{01}^0(\tilde{T}_{i1} | A_i) \exp(\mathbf{X}_i^t \boldsymbol{\beta}_{01}^{A_i}) + H_{02}^0(\tilde{T}_{i1} | A_i) \exp(\mathbf{X}_i^t \boldsymbol{\beta}_{02}^{A_i}) \right) + \right. \right. \\
&\quad \left. \left. \left((H_{12}^0(\tilde{T}_{i2} | A_i) - H_{12}^0(\tilde{T}_{i1} | A_i)) \exp(\mathbf{X}_i^t \boldsymbol{\beta}_{12}^{A_i}) \delta_1 \right) \right] \right\} f(\gamma_{A_i}) d\gamma_{A_i} \\
&= \lambda'_i \int_0^\infty \gamma_{A_i}^{\delta'_i} \exp(-\gamma_{A_i} k_i) \frac{\gamma_{A_i}^{1/\theta_{A_i}-1} \exp(-(1/\theta_{A_i})\gamma_{A_i})}{\Gamma(1/\theta_{A_i}) \theta_{A_i}^{1/\theta_{A_i}}} d\gamma_{A_i}, \tag{A.24}
\end{aligned}$$

where

$$\begin{aligned}
\lambda'_i &= \exp \left(\delta_{i1} X_i^t \boldsymbol{\beta}_{01}^{A_i} + (1 - \delta_{i1}) \delta_{i2} X_i^t \boldsymbol{\beta}_{02}^{A_i} + \delta_{i1} \delta_{i2} X_i^t \boldsymbol{\beta}_{12}^{A_i} \right) \left[\lambda_{01}^0(\tilde{T}_{i1} | A_i) \right]^{\delta_{i1}} \left[\lambda_{02}^0(\tilde{T}_{i2} | A_i) \right]^{(1-\delta_{i1})\delta_{i2}} \left[\lambda_{12}^0(\tilde{T}_{i2} | A_i) \right]^{\delta_{i1}\delta_{i2}}, \\
\delta'_i &= \delta_{i1} + \delta_{i2}, \text{ and} \\
k_i &= H_{01}^0(\tilde{T}_{i1} | A_i) \exp(\mathbf{X}_i^t \boldsymbol{\beta}_{01}^{A_i}) + H_{02}^0(\tilde{T}_{i1} | A_i) \exp(\mathbf{X}_i^t \boldsymbol{\beta}_{02}^{A_i}) + [H_{12}^0(\tilde{T}_{i2} | A_i) - H_{12}^0(\tilde{T}_{i1} | A_i)] \exp(\mathbf{X}_i^t \boldsymbol{\beta}_{12}^{A_i}) \delta_{i1}.
\end{aligned}$$

Define $\alpha'_i = \frac{1}{\theta} + \delta'_i$. Now, the term in (A.24) can be written as

$$\begin{aligned}
& \lambda'_i \frac{\Gamma(\alpha'_i) \theta_{A_i}^{\alpha'_i}}{\Gamma(1/\theta_{A_i}) \theta_{A_i}^{1/\theta_{A_i}}} \int_0^\infty \frac{\gamma_{A_i}^{\alpha'_i-1} \exp(-(1/\theta_{A_i})\gamma_{A_i})}{\Gamma(\alpha'_i) \theta_{A_i}^{\alpha'_i}} \exp(-k_i \gamma_{A_i}) d\gamma_{A_i} \\
&= \lambda'_i \frac{\Gamma(\alpha'_i)}{\Gamma(1/\theta_{A_i})} \cdot \theta_{A_i}^{\delta'_i} E_{G_i}[\exp(-k_i G_i)] \\
&= \lambda'_i \frac{\Gamma(\alpha'_i)}{\Gamma(1/\theta_{A_i})} \cdot \theta_{A_i}^{\delta'_i} LP_{G_i}(k_i), \tag{A.25}
\end{aligned}$$

where for every i , G_i is a Gamma random variable, with a shape parameter α'_i and a scale parameter θ_{A_i} , and $LP_\omega(v) = E_\omega[\exp(-v\omega)]$ is the Laplace transform of a Gamma random variable ω , at the point v . Now, plugging the Laplace transform of a Gamma random variable, (A.25) can be replaced by

$$\begin{aligned}
&= \lambda'_i \frac{\Gamma(\alpha'_i)}{\Gamma(1/\theta_{A_i})} \cdot \theta_{A_i}^{\delta'_i} \left[\frac{1/\theta_{A_i}}{k_i + 1/\theta_{A_i}} \right]^{\alpha'_i} \\
&= \lambda'_i \frac{\Gamma(\alpha'_i)}{\Gamma(1/\theta_{A_i})} \cdot \left[\frac{\theta_{A_i}}{1 + \theta_{A_i} k_i} \right]^{\delta'_i} [1 + \theta_{A_i} k_i]^{-1/\theta_{A_i}} \\
&= \lambda'_i \frac{\Gamma(1/\theta_{A_i} + \delta'_i)}{\Gamma(1/\theta_{A_i})} \cdot \left[\frac{\theta_{A_i}}{1 + \theta_{A_i} k_i} \right]^{\delta'_i} \phi_{A_i}^{(0)}(k_i), \tag{A.26}
\end{aligned}$$

where for $a = 0, 1$, $q = 0, 1, 2$, $\phi_a^{(q)}(k)$ is the q -th derivative of $LP_{\gamma_a}(k)$, with respect to k .

Using the fact that $\Gamma(u+1) = u\Gamma(u)$, and that $\delta'_i \in \{0, 1, 2\}$ is a non-negative integer, we obtain

$$L_i = \lambda'_i (-1)^{\delta'_i} \phi_{A_i}^{(\delta'_i)}(k_i).$$

Therefore, the likelihood function, marginalized over the frailty distribution, equals to

$$\begin{aligned}
L(\tilde{\boldsymbol{\theta}}, \tilde{\boldsymbol{\Lambda}}_0, \tilde{\boldsymbol{\lambda}}_0, \tilde{\boldsymbol{\beta}}) &= \Pi_{i=1}^n \left\{ \left[\lambda_{01}^0(\tilde{T}_{i1}|A_i) \right]^{\delta_{i1}} \left[\lambda_{02}^0(\tilde{T}_{i1}|A_i) \right]^{(1-\delta_{i1})\delta_{i2}} \left[\lambda_{12}^0(\tilde{T}_{i1}|A_i) \right]^{\delta_{i1}\delta_{i2}} \right. \\
&\quad \left. \exp \left(\delta_{i1} X_i^t \beta_{01}^{A_i} + (1 - \delta_{i1}) \delta_{i2} X_i^t \beta_{02}^{A_i} + \delta_{i1} \delta_{i2} X_i^t \beta_{12}^{A_i} \right) (-1)^{\delta_{i1} + \delta_{i2}} \phi_{A_i}^{(\delta_{i1} + \delta_{i2})}(k_i) \right\}.
\end{aligned}$$

F.2 Expectation maximization algorithm

We implemented the EM algorithm proposed by [Nevo & Gorfine \(2022\)](#) for estimation. First, we set the initial values of $\tilde{\boldsymbol{\beta}}$ and $\tilde{\boldsymbol{\Lambda}}_0(t)$ according to the estimates obtained from standard Cox regression models, with $\gamma_{A_i} = 1$ for each patient $i = 1, \dots, n$. The three steps outlined below were then repeated until convergence.

(a) E-step:

- (i) As shown by [Nevo & Gorfine \(2022\)](#), for each patient $i = 1, \dots, n$, the posterior expectation of γ_{A_i} given the observed data can be written as

$$E[\gamma_{A_i}|D_i] = \frac{(-1)^{\delta'_i+1} \phi_{A_i}^{\delta'_i+1}(k_i)}{(-1)^{\delta'_i} \phi_{A_i}^{\delta'_i}(k_i)},$$

where D_i is the observed data for patient i . For each patient i we then estimated $\hat{E}[\log \gamma_{A_i}|D_i]$ and $\hat{E}[\gamma_{A_i}|D_i]$ using the current values of $\tilde{\beta}$, $\tilde{\Lambda}_0(t)$ (which are both required to obtain k_i) and $\tilde{\theta}$ (which is required for ϕ_0 and ϕ_1).

(b) M-step:

- (i) We estimated $\tilde{\beta}$ with six Cox regression models, with offset terms $\log \hat{E}[\gamma_{A_i}|D_i]$. We estimated $\tilde{\Lambda}_0(t)$ using Breslow estimators.
- (ii) To estimate $\tilde{\theta}$, we estimated θ_a (for $a = 0, 1$) by maximizing the conditional expectation of the estimated log-likelihood of γ_a within treatment group $A = a$, given the observed data and the current parameter values.

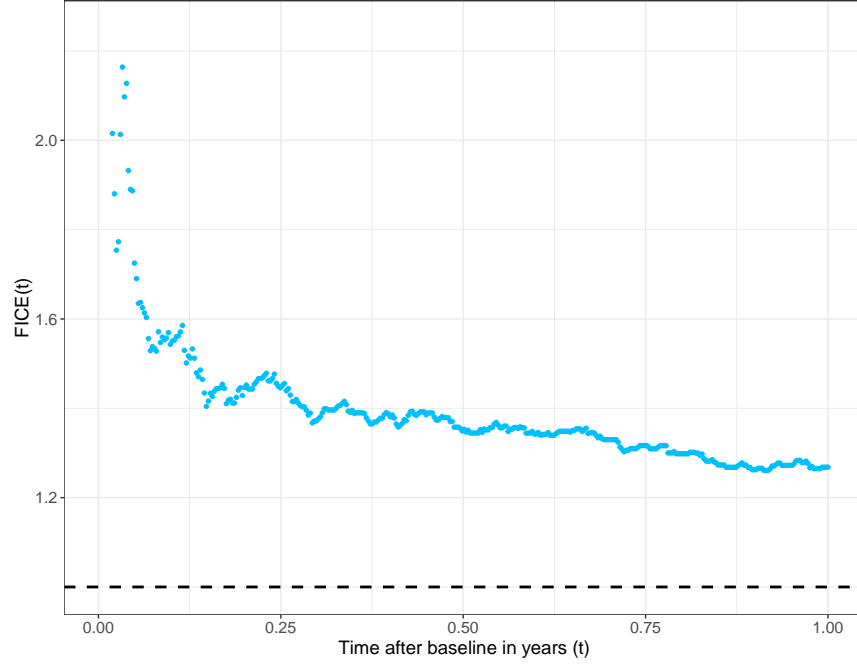
The algorithm adopted to the specific case where the frailty bivariate random variable is Gamma distributed is given in [Nevo & Gorfine \(2022\)](#).

G Application to the motivating example - additional information and figures

G.1 Bounds

Figure [A4](#) below shows the upper bound for the FICE(t) on the risk-ratio scale under weak-ORP. The risk-ratio scale estimand declined over time, from approximately 2.00 two weeks after baseline to 1.27 (CI95%: 1.07, 1.46) after one year.

Figure A4: Estimated upper bounds for the $FICE(t)$ on the risk-ratio scale under weak-ORP and ios-ORP. The bounds under weak-ORP and under ios-ORP coincide analytically. The lower bounds under weak-ORP and without ORP-type assumptions were zero, i.e, non-informative. The upper bound without ORP-type assumptions was also non-informative.



G.2 Analysis under the frailty assumptions

G.2.1 Regression coefficients

Tables A5 and A6 below show the hazard ratio estimates obtained from the hazard models (Equation (2)), with $A = 0$ and $A = 1$, respectively, employed for estimation of the causal effects under the frailty assumptions in Section 6 of the main text. Wald-type 95% confidence intervals, with estimated SEs obtained by Bootstrap, are also reported. When including the sample location variables in the hazard models, their estimated coefficients' SEs were extremely high in transition 12, presumably due to complete (or quasi) separation. Therefore, we did not include these variables in the hazard models for transition 12.

Table A5: Cox regression model estimates for transitions $jk = 01, 02, 12$, within the Access group ($A = 0$). HR: hazard ratio; CI95%: 95% confidence intervals. Cefta: ceftazidime.

Covariate	jk = 01		jk = 02		jk = 12	
	HR	CI	HR	CI	HR	CI
Demographics						
Age	1.01	[0.92, 1.11]	1.12	[0.87, 1.44]	1.44	[0.24, 8.52]
Age ²	1.001	[0.999, 1.003]	0.999	[0.996, 1.003]	0.99	[0.97, 1.02]
Age ³	1.00	[1.00, 1.00]	1.00	[1.00, 1.00]	1.00	[1.00, 1.00]
Male [†]	0.86	[0.64, 1.15]	0.80	[0.64, 1.00]	0.93	[0.44, 1.98]
Sample location at baseline						
Other	1.00		1.00		1.00	
Not taken	1.67	[0.07, 41.56]	0.63	[0.38, 1.04]		
Multiple sources	2.66	[0.10, 69.37]	0.78	[0.44, 1.38]		
Urine	1.83	[0.07, 47.38]	0.86	[0.50, 1.47]		
Wound	1.24	[0.02, 62.67]	0.53	[0.23, 1.24]		
Blood	1.95	[0.01, 307.51]	1.80	[0.96, 3.36]		
Sputum	1.35	[0.02, 75.45]	0.79	[0.38, 1.63]		
Arrived from						
Other	1.00		1.00		1.00	
Home	0.65	[0.41, 1.04]	0.90	[0.62, 1.31]	0.54	[0.15, 1.90]
Institution	1.26	[0.72, 2.19]	1.59	[1.06, 2.39]	0.69	[0.16, 3.09]
Hospitalization unit						
Other	1.00		1.00		1.00	
Internal	1.18	[0.68, 2.06]	1.87	[1.26, 2.76]	5.46	[1.99, 14.98]
Surgical	0.53	[0.29, 0.94]	0.33	[0.22, 0.50]	0.54	[0.03, 9.93]
Medical history						
Dementia	1.18	[0.77, 1.80]	0.84	[0.61, 1.15]	1.11	[0.39, 3.13]
CRF	1.25	[0.81, 1.91]	0.74	[0.55, 0.99]	1.49	[0.61, 3.64]
Immunosuppression	1.08	[0.69, 1.69]	1.68	[1.25, 2.26]	1.38	[0.45, 4.20]
Diabetes	1.45	[1.07, 1.96]	1.10	[0.88, 1.38]	0.90	[0.44, 1.85]
Catheter	2.85	[1.82, 4.46]	2.61	[1.94, 3.52]	1.78	[0.79, 3.98]
Previous antibiotic (any)	1.23	[0.89, 1.71]	1.07	[0.83, 1.38]	2.07	[0.85, 5.04]
Previous cefta culture (365 days) [†]	1.65	[1.08, 2.53]	2.01	[1.42, 2.83]	0.29	[0.08, 1.10]
Medical information						
Arrival to culture (> 2 days) [†]	2.59	[1.75, 3.82]	0.69	[0.52, 0.91]	0.75	[0.33, 1.70]
Arrival to treatment (> 2 days) [†]	1.05	[0.68, 1.62]	1.15	[0.82, 1.60]	1.49	[0.64, 3.46]

[†] Male is an indicator variable denoting whether the patient is a male. Arrival to culture and Arrival to treatment are indicators for whether arrival preceded culture collection or antibiotic treatment initiation, respectively, by more than two days. Previous ceftazidime culture is an indicator variable denoting whether a ceftazidime culture was taken before baseline.

Table A6: Cox regression model estimates for transitions $jk = 01, 02, 12$, within the Watch group ($A=1$). HR: hazard ratio; CI95%: 95% confidence intervals. Cefta: ceftazidime.

Covariate	jk = 01		jk = 02		jk = 12	
	HR	CI	HR	CI	HR	CI
Demographics						
Age	1.05	[0.98, 1.12]	1.41	[1.08, 1.84]	1.10	[0.66, 1.84]
Age ²	1.00	[0.999, 1.001]	0.996	[0.992, 0.999]	0.999	[0.991, 1.001]
Age ³	1.00	[1.00, 1.00]	1.00	[1.00, 1.00]	1.00	[1.00, 1.00]
Male [†]	1.09	[0.87, 1.37]	0.82	[0.68, 0.98]	0.90	[0.52, 1.56]
Sample location at baseline						
Other	1.00		1.00		1.00	
Not taken	1.18	[0.55, 2.51]	0.40	[0.26, 0.62]		
Multiple sources	1.37	[0.57, 3.28]	0.48	[0.30, 0.77]		
Urine	1.67	[0.79, 3.53]	0.34	[0.21, 0.55]		
Wound	1.06	[0.43, 2.63]	0.54	[0.29, 0.99]		
Blood	2.34	[0.97, 5.62]	0.67	[0.36, 1.23]		
Sputum	1.04	[0.30, 3.60]	0.49	[0.25, 0.95]		
Arrived from						
Other	1.00		1.00		1.00	
Home	0.65	[0.44, 0.96]	0.88	[0.62, 1.24]	1.47	[0.52, 4.17]
Institution	1.44	[0.88, 2.36]	1.25	[0.85, 1.85]	3.59	[1.11, 11.57]
Hospitalization unit						
Other	1.00		1.00		1.00	
Internal	1.00	[0.68, 1.46]	0.69	[0.51, 0.94]	1.12	[0.46, 2.72]
Surgical	1.37	[0.91, 2.08]	0.21	[0.14, 0.31]	0.38	[0.14, 1.02]
Medical history						
Dementia	1.23	[0.86, 1.74]	0.80	[0.59, 1.09]	0.40	[0.18, 0.89]
CRF	1.08	[0.77, 1.51]	1.04	[0.76, 1.41]	2.02	[1.03, 3.93]
Immunosuppression	1.58	[1.14, 2.19]	1.49	[1.13, 1.96]	2.07	[1.08, 3.99]
Diabetes	1.19	[0.92, 1.53]	0.81	[0.65, 1.01]	1.47	[0.93, 2.33]
Catheter	1.95	[1.42, 2.68]	2.11	[1.61, 2.77]	1.03	[0.47, 2.27]
Previous antibiotic (any)	1.33	[1.03, 1.72]	1.27	[1.02, 1.58]	1.51	[0.75, 3.04]
Previous cefta culture (365 days) [†]	1.04	[0.73, 1.49]	1.46	[1.10, 1.94]	1.30	[0.60, 2.79]
Medical information						
Arrival to culture (> 2 days) [†]	3.23	[2.44, 4.28]	0.80	[0.62, 1.03]	1.91	[1.04, 3.52]
Arrival to treatment (> 2 days) [†]	0.83	[0.62, 1.10]	0.93	[0.72, 1.19]	0.93	[0.46, 1.89]

[†] Male is an indicator variable denoting whether the patient is a male. Arrival to culture and Arrival to treatment are indicators for whether arrival preceded culture collection or antibiotic treatment initiation, respectively, by more than two days. Previous ceftazidime culture is an indicator variable denoting whether a ceftazidime culture was taken before baseline.

G.2.2 Data analysis under different ρ values

Figure A5 depicts the estimated causal effects under the frailty assumptions for ρ values different than zero. The results did not differ substantially from those presented in Section 6 of the main text, although the FICE(t) remained non-significantly different from zero for a more extended period.

Figure A5: Comparison between estimates of the different estimands within one year after baseline under the frailty assumptions with $\rho = 0.5$ (first figure) and $\rho = 1$ (second figure). The upper panel of each figure shows the various estimates on the difference scale. The lower panel shows the various estimates on the risk-ratio scale.

